

OPTIMAL QUADRATIC ELEMENT ON RECTANGULAR GRIDS FOR H^1 PROBLEMS

HUILAN ZENG, CHENSONG ZHANG, AND SHUO ZHANG

ABSTRACT. In this paper, a piecewise quadratic finite element method on rectangular grids for H^1 problems is presented. The proposed method can be viewed as a reduced rectangular Morley (RRM) element. For the source problem, the convergence rate of this scheme is proved to be $O(h^2)$ in the energy norm on uniform grids over a convex domain. A lower bound of the L^2 -norm error is also proved, which makes the capacity of this scheme more clear. For the eigenvalue problem, the computed eigenvalues by this element are shown to be the lower bounds of the exact ones. Some numerical results are presented to verify the theoretical findings.

1. INTRODUCTION

The design and capacity analysis of the discretization schemes for the source problem (say, the boundary value problem) and the eigenvalue problem are key issues in numerical analysis and, in general, of approximation theory. When the approximation of functions in Sobolev spaces is performed using piecewise polynomials defined on a domain partition, lower-degree polynomials are often preferred in order to achieve a simpler interior structure. A finite element scheme with polynomials of the total degree no more than k , denoted by P_k , is called optimal if it achieves $O(h^{k+1-m})$ accuracy in the energy norm for H^m elliptic problems. In this paper, we present an optimal quadratic element scheme for the H^1 problems, including the source problem and the eigenvalue problem, on rectangular grids, and present its error analysis.

The study of optimal finite element schemes has been attracting wide interests. For the case wherein the grid comprises simplexes, there are already some systematic results. It is known that the Lagrange finite elements of arbitrary degree on domains of arbitrary dimension are optimal conforming elements for second-order elliptic problems. At the same time, a systematic family of minimal-degree nonconforming finite elements is proposed by [27], where m -th degree polynomials work for $2m$ -th order elliptic problems in R^n for any $n \geq m$. Known as the Wang-Xu

2000 *Mathematics Subject Classification.* Primary 65N15, 65N22, 65N25, 65N30.

Key words and phrases. optimal quadratic element, rectangular grids, boundary value problem, eigenvalue problem, lower bound.

Zeng and C.-S. Zhang are partially supported by National Key Research and Development Program 2016YFB0201304, China. C.-S. Zhang is also supported by the Key Research Program of Frontier Sciences of CAS. S. Zhang is partially supported by National Natural Science Foundation, 11471026 and 11871465, China.

or Morley-Wang-Xu family, these elements are constructed based on the perfect matching between the dimension of m -th degree polynomials and the dimension of $(n - k)$ -subsimplexes with $1 \leq k \leq m$. The generalisation to the cases where $n < m$ is attracting increasing research interest (see, e.g., [29]). These spaces can be naturally used for both the source problem and the eigenvalue problem. On the other hand, to clarify the capacity of the schemes clearly, some kinds of extremal analysis have also been conducted, including, e.g., lower bounds of the error estimates and guaranteed bounds of the computed eigenvalues. We refer to, e.g., [20] for a general analysis of the lower bounds of the discretization error for piecewise polynomials, and [10-12, 22] for specific analysis with certain finite element schemes. We refer to, e.g., [1, 4, 5, 9, 17, 18, 21, 33, 34, 37] for the computed guaranteed bounds of certain eigenvalue problems. The extremal analysis is naturally used on or ready to be generalized to optimal schemes.

When the grid comprises shapes other than simplexes, the design of optimal schemes becomes more complicated. We would like to recall that, Q_k (rather than P_k) polynomials are used for $2k$ -th order problems on \mathbb{R}^n rectangular grids by [14], which form minimal *conforming* element spaces. For biharmonic equation, some low-degree rectangular elements have been designed, including the rectangular Morley element and incomplete P_3 element. Very recently, a space, consisting of exactly piecewise quadratic polynomials, is constructed and shown convergent for the biharmonic equation on general quadrilateral grids, which forms a convergent scheme of the minimal degree [36]. Also, there have been several rectangle elements for H^1 problems in the literature [13, 15, 16, 28]. In [16], an enriched quadratic nonconforming element on rectangles is introduced, and second-order error is shown, which is generalized to higher orders by [13]. Another second-order quadratic element is given by [15], where the spline technique is used, but the shape function space on a cell is not exactly P_2 . The Wilson element [28] is the first quadratic quadrilateral nonconforming element. Despite its superior performance in practice, as shown in [25], its global asymptotic convergence rate is the same as that of the bilinear element, due to low internal continuity. Generally, this deficiency can be compensated by equipping the piecewise quadratic polynomial with second order moment-continuity across the internal edges. In this way, the moment-continuous (MC) element space is defined. However, it is proved in Appendix A, that the MC element space possesses essentially the same accuracy as that of the bilinear element space, and thus it fails to reach second-order convergence rate. To our best knowledge, it remains open whether an optimal scheme can be constructed with degrees higher than minimal even on rectangular grids and for H^1 problems.

In this paper, we study the optimal finite element construction for the H^1 problems, and present a finite element space comprising piecewise quadratic polynomials on uniform rectangular grids that can provide $O(h^2)$ convergence in energy norm for the source and eigenvalue problems. The

computed eigenvalues are lower bounds of the exact ones, which can be proved theoretically and verified numerically. Only rectangular grids are taken into consideration herein, but if a quadrilateral grid is only a sufficiently small perturbation of a uniform one, then an optimal convergence rate could be expected on it. Moreover, the finite element functions cannot be described with free rein cell by cell. Similar to the elements described in [7, 23, 36] and in many spline-type methods, the number of continuity restrictions of the finite element function is greater than the dimension of the local polynomial space. We believe this difficulty is not abnormal for low-degree schemes. In general, these cells can share interfaces with more neighbour cells, and more continuity restrictions will strengthen the requirement for higher-degree polynomials, generally higher than the order of the underlying Sobolev space. Thus, constructing consistent finite elements in the formulation of Ciarlet's triple is difficult with m -th degree polynomials for H^m problems even on rectangular grids. Here we utilize some non-standard technical approaches to overcome the difficulty for both implementation and especially theoretical analysis.

The main difficulty is that the local interpolation is too difficult, if ever possible, to be established, which plays a fundamental role in the approximation error analysis for the source problem and the guaranteed bounds analysis for the eigenvalue problem. Notice that the space constructed herein can be viewed as a reduced rectangular Morley element space. Similar to the approach in [36] but with technical modifications, we can determine that the finite element functions are discrete stream functions of the discrete divergence-free functions constructed in a study [23]; using this exact relation, we can perform the approximation estimation indirectly. Also, the discretization of the eigenvalue problem can be viewed as an inner approximation of the rectangular Morley element scheme, and this helps avoid the direct dependence on an interpolation. This newly-designed routine method of theoretical analysis can be potentially used to find out other optimal schemes.

Finally, we remark that, two examples, namely the rectangular Morley (RM) element and the reduced rectangular Morley (RRM) element, are reported in this paper that when used for the eigenvalue problem, errors of the eigenvalues and eigenfunctions are of the same order. This unusual performance is due to the fact that no nontrivial conforming finite element subspace can be found contained in these two spaces.

The rest of the paper is organized as follows. In Section 2, some preliminaries are given and some related low-degree rectangle elements are reviewed. In Section 3, the rectangular Morley element is revisited. In Section 4, a reduced rectangular Morley element scheme is presented for both source problem and eigenvalue problem. In Section 5, the convergence analysis and lower bound properties are shown for the RRM element scheme. In Section 6, some concluding remarks and discussions are given. In contrast to a general implementation approach in Section 5, concise sets of basis functions of the MC element and the RRM element are presented in the appendix.

2. PRELIMINARIES

2.1. Notations. Throughout this paper, we use Ω for a simply-connected polygonal domain in \mathbb{R}^2 . We use ∇ , curl , div , and ∇^2 for the gradient operator, curl operator, divergence operator, and Hessian operator, respectively. As usual, we use $H^2(\Omega)$, $H_0^2(\Omega)$, $H^1(\Omega)$, $H_0^1(\Omega)$, and $L^2(\Omega)$ for certain Sobolev spaces. Specifically, we denote $L_0^2(\Omega) := \{w \in L^2(\Omega) : \int_{\Omega} w dx = 0\}$, $\underline{H}_0^1(\Omega) := (H_0^1(\Omega))^2$, and $\underline{H}_n^1(\Omega) := \{v \in (H^1(\Omega))^2 : v \cdot \mathbf{n}|_{\partial\Omega} = 0\}$. Denote, by $\underline{H}^{-1}(\Omega)$ and $H^{-1}(\Omega)$, the dual spaces of $\underline{H}_0^1(\Omega)$ and $H_0^1(\Omega)$, respectively. We use “ $\underline{\cdot}$ ” for vector valued quantities in the present paper, and \underline{v}^1 and \underline{v}^2 for the two components of the function v . We utilize the subscript “ \cdot_h ” to indicate the dependence on grids. Particularly, an operator with the subscript “ \cdot_h ” implies the operation is done cell by cell. Finally, \lesssim , \gtrsim , and \approx respectively denote \leq , \geq , and $=$ up to a generic positive constant, which might depend on the shape-regularity of subdivisions, but not on the mesh-size h [30].

Let \mathcal{G}_h be in a regular family of quadrilateral grids of domain Ω . Let \mathcal{N}_h be the set of all vertices, $\mathcal{N}_h = \mathcal{N}_h^i \cup \mathcal{N}_h^b$, with \mathcal{N}_h^i and \mathcal{N}_h^b comprising the interior vertices and the boundary vertices, respectively. Similarly, let $\mathcal{E}_h = \mathcal{E}_h^i \cup \mathcal{E}_h^b$ be the set of all the edges, with \mathcal{E}_h^i and \mathcal{E}_h^b comprising the interior edges and the boundary edges, respectively. For an edge e , \mathbf{n}_e is a unit vector normal to e and $\boldsymbol{\tau}_e$ is a unit tangential vector of e such that $\mathbf{n}_e \times \boldsymbol{\tau}_e > 0$. On the edge e , we use $[[\cdot]]_e$ for the jump across e . If $e \subset \partial\Omega$, then $[[\cdot]]_e$ is the evaluation on e . The subscript \cdot_e can be dropped when there is no ambiguity brought in.

2.2. Some rectangular finite element spaces. Suppose that $K \subset \mathbb{R}^2$ represents a rectangle with sides parallel to the two axis respectively. Let (x_K, y_K) be the barycenter of K . Let $h_{x,K}$, $h_{y,K}$ be the length of K in the x and y directions, respectively. Let a_i and e_i denote an vertex and an edge of K , respectively. Let $h := \max_{K \in \mathcal{G}_h} \max\{h_{x,K}, h_{y,K}\}$ be the mesh size of \mathcal{G}_h . When \mathcal{G}_h is uniform, we denote $h_x := h_{x,K}$ and $h_y := h_{y,K}$. Let $P_l(K)$ denote the space of polynomials on K of total degree no bigger than l . Let $Q_l(K)$ denote the space of polynomials of degree no bigger than l in each variable. Similarly, we define spaces $P_l(e)$ and $Q_l(e)$ on an edge e .

2.2.1. The Q_1 element. The Q_1 element is defined by $(K, P_K^{\text{BL}}, D_K^{\text{BL}})$ with the following properties:

- (a) K is a rectangle;
- (b) $P_K^{\text{BL}} = Q_1(K)$;
- (c) for any $v \in H^1(K)$, $D_K^{\text{BL}} = \{v(a_i)\}_{i=1:4}$.

Define the Q_1 element space as

$$V_h^{\text{BL}} := \{w_h \in H^1(\Omega) : w_h|_K \in Q_1(K), \forall K \in \mathcal{G}_h\}.$$

Associated with $H_0^1(\Omega)$, we define $V_{h0}^{\text{BL}} := \{w_h \in V_h^{\text{BL}} : w_h(a) = 0, \forall a \in \mathcal{N}_h^b\}$.

2.2.2. The Park–Sheen (PS) element. The PS element [23] is a piecewise linear nonconforming finite element space for H^1 problems. It is defined as

$$V_h^{\text{PS}} := \{w_h \in L^2(\Omega) : w_h|_K \in P_1(K), \forall K \in \mathcal{G}_h, \text{ and } \int_e \llbracket w_h \rrbracket ds = 0, \forall e \in \mathcal{E}_h^i\}.$$

Associated with $H_0^1(\Omega)$, we define $V_{h0}^{\text{PS}} := \{w_h \in V_h^{\text{PS}} : \int_e w_h ds = 0, \forall e \in \mathcal{E}_h^b\}$.

2.2.3. The rotated Q_1 (Q_1^{rot}) element. The Q_1^{rot} element is defined by $(K, P_K^{\text{rQ}}, D_K^{\text{rQ}})$ with the following properties:

- (a) K is a rectangle;
- (b) $P_K^{\text{rQ}} = P_1(K) + \text{span}\{x^2 - y^2\}$;
- (c) for any $v \in H^1(K)$, $D_K^{\text{rQ}} = \left\{ \int_{e_i} v ds \right\}_{i=1:4}$.

Define the Q_1^{rot} element space as

$$V_h^{\text{rQ}} := \{w_h \in L^2(\Omega) : w_h|_K \in P_K^{\text{rQ}}, \forall K \in \mathcal{G}_h, \text{ and } \int_e \llbracket w_h \rrbracket ds = 0, \forall e \in \mathcal{E}_h^i\}.$$

Associated with $H_0^1(\Omega)$, we define $V_{h0}^{\text{rQ}} := \{w_h \in V_h^{\text{rQ}} : \int_e w_h ds = 0, \forall e \in \mathcal{E}_h^b\}$.

2.2.4. The Lin–Tobiska–Zhou (LTZ) element. The LTZ element ([19, 35]) is defined by $(K, P_K^{\text{LTZ}}, D_K^{\text{LTZ}})$ with the following properties:

- (a) K is a rectangle;
- (b) $P_K^{\text{LTZ}} = P_1(K) + \text{span}\{x^2, y^2\}$;
- (c) for any $v \in H^1(K)$, $D_K^{\text{LTZ}} = \left\{ \int_K v dx dy, \int_{e_1} v ds, \dots, \int_{e_4} v ds \right\}$.

Define the LTZ element space as

$$V_h^{\text{LTZ}} := \{w_h \in L^2(\Omega) : w_h|_K \in P_K^{\text{LTZ}}, \forall K \in \mathcal{G}_h, \text{ and } \int_e \llbracket w_h \rrbracket ds = 0, \forall e \in \mathcal{E}_h^i\}.$$

Associated with $H_0^1(\Omega)$, we define $V_{h0}^{\text{LTZ}} := \{w_h \in V_h^{\text{LTZ}} : \int_e w_h ds = 0, \forall e \in \mathcal{E}_h^b\}$, and associated with $H_{\mathbf{n}}^1(\Omega)$, we define $V_{h\mathbf{n}}^{\text{LTZ}} := \{y_h \in (V_h^{\text{LTZ}})^2 : \int_e y_h \cdot \mathbf{n} = 0, \forall e \in \mathcal{E}_h^b\}$.

2.2.5. *The Wilson element.* The Wilson element is defined by (K, P_K^W, D_K^W) with the following properties:

- (a) K is a rectangle;
- (b) $P_K^W = P_2(K)$;
- (c) for any $v \in H^2(K)$, $D_K^W = \{v(a_1), \dots, v(a_4), \int_K \partial_{xx} v dx dy, \int_K \partial_{yy} v dx dy\}$.

Define the Wilson element space as

$$V_h^W := \{w_h \in L^2(\Omega) : w_h|_K \in P_K^W, \forall K \in \mathcal{G}_h, \text{ and } w_h \text{ is continuous at any } a \in \mathcal{N}_h^i\}.$$

Associated with $H_0^1(\Omega)$, we define $V_{h0}^W := \{w_h \in V_h^W : w_h(a) = 0, \forall a \in \mathcal{N}_h^b\}$.

2.2.6. *The moment-continuous (MC) element.* Associated with \mathcal{G}_h , the MC element space is defined as

$$V_h^{\text{MC}} := \{w_h \in L^2(\Omega) : w_h|_K \in P_2(K), \text{ and } w_h \text{ is moment-continuous on } \mathcal{G}_h\}.$$

Associated with $H_0^1(\Omega)$, we define

$$V_{h0}^{\text{MC}} := \{w_h \in V_h^{\text{MC}} : w_h \text{ is moment-homogeneous on } \mathcal{G}_h\}.$$

A piecewise quadratic polynomial function w is moment-continuous of second-order, if

$$\int_e \llbracket w \rrbracket_e v ds = 0, \forall v \in P_1(e), e \in \mathcal{E}_h^i.$$

Moreover, w is moment-homogeneous of second-order, if $\int_e w v ds = 0, \forall v \in P_1(e), e \in \mathcal{E}_h^b$.

A piecewise quadratic function v_h belongs to V_{h0}^{MC} if and only if v_h is continuous at the second-order Gauss points of any $e \in \mathcal{E}_h^i$ and vanishes on the Gauss points of any $e \in \mathcal{E}_h^b$.

Theorem 2.1. *If \mathcal{G}_h is a $m \times n$ rectangular subdivision of Ω , then $\dim(V_{h0}^{\text{MC}}) = 2mn - m - n + 1$.*

Theorem 2.2. *If \mathcal{G}_h be a $m \times n$ rectangular subdivision of Ω , then $\dim(V_h^{\text{MC}}) = 2mn + 2m + 2n$.*

Detailed proof of Theorems 2.1 and 2.2 are put in Appendix A, and available sets of basis functions of V_{h0}^{MC} and V_h^{MC} are also presented there.

2.3. **Some technical lemmas.** In addition to these spaces above, we denote

$$\begin{aligned}\mathcal{L}_h^0 &:= \{q \in L^2(\Omega) : q|_K \in P_0(K)\}, & \mathcal{L}_{h0}^0 &:= \mathcal{L}_h^0 \cap L_0^2(\Omega), \\ \underline{V}_{hm}^{\text{BL}} &:= \{\underline{v} \in (V_h^{\text{BL}})^2 : \underline{v} \cdot \mathbf{n}|_{\partial\Omega} = 0\}, & \underline{V}_{hm}^{\text{rQ}} &:= \{\underline{v} \in (V_h^{\text{rQ}})^2 : \int_e \underline{v} \cdot \mathbf{n} = 0, \forall e \in \mathcal{E}_h^b\}, \\ \underline{V}_{hm}^{\text{PS}} &:= (V_h^{\text{PS}})^2 \cap \underline{V}_{hm}^{\text{rQ}}, & \underline{V}_{hm}^{\text{LTZ}} &:= \{\underline{v} \in (V_h^{\text{LTZ}})^2 : \int_e \underline{v} \cdot \mathbf{n} = 0, e \in \mathcal{E}_h^b\}.\end{aligned}$$

Let Π_h^{rQ} and $\underline{\Pi}_h^{\text{rQ}}$ be the nodal interpolation associated with V_h^{rQ} and $(V_h^{\text{rQ}})^2$, respectively.

Lemma 2.3. ([24, Lemma 1], [36, Lemma 6]) *For the Q_1^{rot} element, we have*

- (1) $|\Pi_h^{\text{rQ}} v|_{1,h} \lesssim |v|_{1,h}, \forall v \in H_0^1(\Omega) \cap H^2(\Omega);$
- (2) $\|\Pi_h^{\text{rQ}} v - v\|_{0,\Omega} + h|\Pi_h^{\text{rQ}} v - v|_{1,h} \lesssim h^2 |v|_{2,\Omega}, \forall v \in H_0^1(\Omega) \cap H^2(\Omega).$

Lemma 2.4. ([36, Lemma 7]) *The following relationships hold.*

$$\Pi_h^{\text{rQ}} V_h^{\text{BL}} = V_h^{\text{PS}} \quad \text{and} \quad \underline{\Pi}_h^{\text{rQ}} \underline{V}_{hm}^{\text{BL}} = \underline{V}_{hm}^{\text{PS}}.$$

2.4. **H^1 elliptic problems and nonconforming finite element approximation.** In this paper, we consider the following model problems:

- Source problem: with $f \in Q := L^2(\Omega)$, $\rho \in L^\infty(\Omega)$, and $\rho \geq c_0 > 0$,

$$(2.1) \quad \begin{cases} -\Delta u = \rho f & \text{in } \Omega, \\ u = 0 & \text{on } \partial\Omega. \end{cases}$$

Its weak form is given by: Find $u \in V := H_0^1(\Omega)$ satisfying

$$(2.2) \quad a(u, v) = b(f, v), \quad \forall v \in V,$$

where $a(u, v) = \int_\Omega \nabla u \cdot \nabla v \, dx dy$ and $b(f, v) = \int_\Omega \rho f v \, dx dy$.

- Eigenvalue problem: with $\rho \in L^\infty(\Omega)$ and $\rho \geq c_0 > 0$,

$$(2.3) \quad \begin{cases} -\Delta u = \lambda \rho u & \text{in } \Omega, \\ u = 0 & \text{on } \partial\Omega. \end{cases}$$

Its weak form is given by: Find $(\lambda, u) \in \mathbb{R} \times V$ with $\|u\|_{0,\rho} = 1$, such that

$$(2.4) \quad a(u, v) = \lambda b(u, v), \quad \forall v \in V,$$

where $\|v\|_{0,\rho} := b(v, v)^{\frac{1}{2}}$ defines a norm over V equivalent to the usually L^2 norm.

From [2], the eigenvalue problem (2.3) has a sequence of eigenvalues

$$0 < \lambda_1 \leq \lambda_2 \leq \cdots \leq \lambda_k \leq \cdots, \text{ satisfying } \lim_{k \rightarrow \infty} \lambda_k = \infty,$$

and corresponding eigenfunctions

$$u_1, u_2, \cdots, u_k, \cdots, \text{ satisfying } b(u_i, u_j) = \delta_{ij}.$$

For a certain eigenvalue λ_j of (2.4), we define

$$M(\lambda_j) = \{w \in V : w \text{ is an eigenfunction of (2.4) corresponding to } \lambda_j\}.$$

Given an discrete space V_h defined on \mathcal{G}_h , the discretization schemes are

• for the source problem: Find $u_h \in V_h$, such that

$$(2.5) \quad a_h(u_h, v_h) = b(f, v_h), \quad \forall v_h \in V_h,$$

• for the eigenvalue problem: Find $(\lambda_h, u_h) \in \mathbb{R} \times V_h$ with $\|u_h\|_{0,\rho} = 1$, such that

$$(2.6) \quad a_h(u_h, v_h) = \lambda_h b(u_h, v_h), \quad \forall v_h \in V_h.$$

Let $\dim V_h = N$. The discrete eigenvalue problem (2.6) has a sequence of eigenvalues

$$0 < \lambda_{1,h} \leq \lambda_{2,h} \leq \cdots \leq \lambda_{N,h},$$

and corresponding eigenfunctions

$$u_{1,h}, u_{2,h}, \cdots, u_{N,h}, \text{ satisfying } b(u_{i,h}, u_{j,h}) = \delta_{ij}.$$

Lemma 2.5. ([6, Theorem 4.1.7]) *Suppose that Ω is a rectangular region and ρ is smoothing enough. If (λ_j, u_j) is an eigen-pair of (2.3), then $u_j \in C^{5,\alpha}(\Omega)$.*

3. THE RECTANGULAR MORLEY (RM) ELEMENT REVISITED

3.1. The RM element space. The RM element is defined by (K, P_K^M, D_K^M) with the following properties:

- (1) K is a rectangle;
- (2) $P_K^M = P_2(K) + \text{span}\{x^3, y^3\}$;
- (3) for any $v \in H^2(K)$, $D_K^M = \{v(a_i), \int_{e_i} \partial_{n_{e_i}} v ds\}_{i=1:4}$.

Define the RM element space as

$$V_h^M := \{w_h \in L^2(\Omega) : w_h|_K \in P_K^M, w_h(a) \text{ is continuous at any } a \in \mathcal{N}_h^i,$$

$$\text{and } \int_e \partial_{n_e} w_h ds \text{ is continuous across any } e \in \mathcal{E}_h^i\}.$$

Associated with $H_0^1(\Omega)$, we define $V_{hs}^M := \{w_h \in V_h^M : w_h(a) = 0, \forall a \in \mathcal{N}_h^b\}$.

Lemma 3.1. ([22, Lemmas 3.2 and 3.5]) Denote $E_h(w, v_h) := a_h(w, v_h) + (\Delta w, v_h)$ with $w \in V$ and $v_h \in V_h$. The following estimates hold.

(a) For any shape-regular rectangular grid, it holds for any $v_h \in V_{hs}^M$ that

$$|E_h(v, v_h)| \lesssim \sum_{K \in \mathcal{G}_h} h_K^2 |v|_{2,K} |v_h|_{2,K} \lesssim h |v|_{2,\Omega} |v_h|_{1,h}, \quad \forall v \in H^2(\Omega) \cap H_0^1(\Omega).$$

(b) For any uniform rectangular grid, it holds for any $v_h \in V_{hs}^M$ that

$$|E_h(v, v_h)| \lesssim h^{k-1} |v|_{k,\Omega} |v_h|_{1,h}, \quad \forall v \in H^k(\Omega) \cap H_0^1(\Omega), \quad k = 2, 3.$$

For the RM element, there is a refined property of the interpolation operator $\Pi_h^M : V \mapsto V_{hs}^M$.

Lemma 3.2. ([22, Lemma 3.17]) Assume that \mathcal{G}_h is uniform. For any $w \in H_0^1(\Omega) \cap H^3(\Omega)$ with $\|\frac{\partial^2 w}{\partial x \partial y}\|_{0,\rho} \neq 0$, if h is small enough, then

$$(3.1) \quad a_h(w - \Pi_h^M w, \Pi_h^M w) \geq \alpha h^2,$$

where $\alpha > 0$ is a constant independent of h .

Corollary 3.3. Under the conditions in Lemma 3.2, there exists $\alpha_1 > 0$, such that

$$(3.2) \quad a_h(w - \Pi_h^M w, w) \geq \alpha_1 h^2.$$

Proof. It follows from Lemma 3.2 and $|w - \Pi_h^M w|_{1,h} \lesssim h^2$ immediately. \square

Hence we obtain an interesting and intuitive conclusion:

$$(3.3) \quad a_h(u - \Pi_h^M u, u) \approx |u - \Pi_h^M u|_{1,h} |u|_{1,h}, \quad \text{when } h \text{ is small enough.}$$

By standard argument, we can prove the exact sequence which reads

$$(3.4) \quad 0 \longrightarrow V_{hs}^M \xrightarrow{\text{curl}_h} \underline{V}_{hm}^{\text{LTZ}} \xrightarrow{\text{div}_h} \mathcal{L}_h^{1,-1} \longrightarrow 0,$$

where $\mathcal{L}_h^{1,-1} = \{q \in L_0^2(\Omega) : q|_K \in P_1(K)\}$.

3.2. The RM element scheme for the H^1 eigenvalue problem.

3.2.1. *Expanded representation of the difference between energy of states.* Simple calculations yield

$$(3.5) \quad \begin{aligned} a(v_1, v_1) + a_h(v_2, v_2) &= 2a_h(v_1, v_2) + a_h(v_1 - v_2, v_1 - v_2) \\ &= 2a_h(v_3, v_2) + 2a_h(v_1 - v_3, v_3) \\ &\quad + 2a_h(v_1 - v_3, v_2 - v_3) + a_h(v_1 - v_2, v_1 - v_2), \end{aligned}$$

$$(3.6) \quad \begin{aligned} a_h(v_2, v_2) - a(v_1, v_1) &= [2a_h(v_3, v_2) - 2a(v_1, v_1)] + 2a_h(v_1 - v_3, v_3) \\ &\quad + 2a_h(v_1 - v_3, v_2 - v_3) + a_h(v_1 - v_2, v_1 - v_2), \end{aligned}$$

$$(3.7) \quad \begin{aligned} a(v_1, v_1) - a_h(v_2, v_2) &= 2a_h(v_3 - v_2, v_2) + 2a_h(v_1 - v_3, v_3) \\ &\quad + 2a_h(v_1 - v_3, v_2 - v_3) + a_h(v_1 - v_2, v_1 - v_2). \end{aligned}$$

Let u be the solution of the source problem (2.2) or the eigenvalue problem (2.4) and u_h be its approximation. Let $v_1 = u$, $v_2 = u_h$ and $v_3 = \Pi_h u$, where $\Pi_h : V \mapsto V_{h0}$ is an interpolation operator. We use (3.6) to obtain an expansion of $b(-f, u - u_h)$ and (3.7) to obtain an expansion of $\lambda - \lambda_h$.

- For the source problem:

Let u and u_h be the solutions of (2.2) and (2.5), respectively. It holds that

$$b(-f, u - u_h) = a_h(u_h, u_h) - a(u, u).$$

From $[2a_h(\Pi_h u, u_h) - 2a(u, u)] = 2b(f, \Pi_h u - u)$, the formula (3.6) becomes

$$(3.8) \quad \begin{aligned} a_h(u_h, u_h) - a(u, u) &= 2b(f, \Pi_h u - u) + 2a_h(u - \Pi_h u, \Pi_h u) \\ &\quad + 2a_h(u - \Pi_h u, u_h - \Pi_h u) + a_h(u - u_h, u - u_h), \end{aligned}$$

Analyze the items on the right-hand-side of (3.8). Suppose that $u \in H^3(\Omega) \cap H_0^1(\Omega)$. With the second term $2a_h(u - \Pi_h u, \Pi_h u)$ not considered, the rest items in (3.8) are of high order than $|u - u_h|_{1,h}$. Therefore, $2a_h(u - \Pi_h u, \Pi_h u)$ becomes the dominant factor to determine whether $b(-f, u - u_h)$ is of higher order than $|u - u_h|_{1,h}$.

- For the eigenvalue problem:

Let u and u_h be the solutions of (2.4) and (2.6), which satisfy $b(u, u) = b(u_h, u_h) = 1$. It holds that

$$\lambda - \lambda_h = a(u, u) - a_h(u_h, u_h).$$

Notice that $2b(u_h, u - u_h) = 2b(u_h, u) - b(u_h, u_h) - b(u, u) = -b(u - u_h, u - u_h)$. Thus we can obtain

$$\begin{aligned} 2a_h(\Pi_h u - u_h, u_h) &= 2\lambda_h b(u_h, \Pi_h u - u_h) = 2\lambda_h b(u_h, \Pi_h u - u) + 2\lambda_h b(u_h, u - u_h) \\ &= 2\lambda_h b(u_h, \Pi_h u - u) - \lambda_h b(u - u_h, u - u_h). \end{aligned}$$

Based on these above, (3.7) becomes

$$(3.9) \quad \begin{aligned} a(u, u) - a_h(u_h, u_h) &= 2\lambda_h b(u_h, \Pi_h u - u) - \lambda_h b(u - u_h, u - u_h) + 2a_h(u - \Pi_h u, \Pi_h u) \\ &\quad + 2a_h(u - \Pi_h u, u_h - \Pi_h u) + a_h(u - u_h, u - u_h). \end{aligned}$$

Analyze the items on the right-hand-side of (3.9). Similarly, $2a_h(u - \Pi_h u, \Pi_h u)$ is also the dominant factor to determine whether $\lambda - \lambda_h$ is of higher order than $|u - u_h|_{1,h}$.

3.2.2. *Analysis of the RM element for the eigenvalue problem.* Based on the error estimates of the rectangular Morley element scheme for the source problem (see [22]), the following estimates for the eigenvalue problem follows by standard argument.

Theorem 3.4. *Let λ_j be the j -th eigenvalue of (2.4), and $(\lambda_{j,h}^M, u_{j,h}^M) \in \mathbb{R} \times V_{hs}^M$ be the j -th eigen-pair of (2.6) with $\|u_{j,h}^M\|_{0,\rho} = 1$. It holds that*

(a) *if $M(\lambda_j) \subset H_0^1(\Omega) \cap H^2(\Omega)$, then there exists $u_j \in M(\lambda_j)$ with $\|u_j\|_{0,\rho} = 1$, such that*

$$|\lambda_j - \lambda_{j,h}^M| \lesssim h^2, \quad \|u_j - u_{j,h}^M\|_{0,\rho} \lesssim h^2, \quad \text{and} \quad |u_j - u_{j,h}^M|_{1,h} \lesssim h;$$

(b) *if the mesh is uniform and $M(\lambda_j) \subset H_0^1(\Omega) \cap H^3(\Omega)$, then there exists $u_j \in M(\lambda_j)$ with $\|u_j\|_{0,\rho} = 1$, such that $|u_j - u_{j,h}^M|_{1,h} \lesssim h^2$.*

Moreover, we obtain the lower-bound property of eigenvalue approximations by the RM element.

Theorem 3.5. *Let λ_j and $\lambda_{j,h}^M$ be an exact eigenvalue and its approximation by the RM element. Suppose that $u_j \in H_0^1(\Omega) \cap H^3(\Omega)$ and the mesh is uniform. When h is small enough, we have*

$$(3.10) \quad \lambda_j - \lambda_{j,h}^M \geq C_M h^2.$$

where C_M is a positive constant independent of h .

Proof. We have the basic expansion by [33, 34], which generalizes the identity introduced by [1],

$$(3.11) \quad \begin{aligned} \lambda_j - \lambda_{j,h}^M &= |u_j - u_{j,h}^M|_{1,h}^2 - \lambda_{j,h}^M \|u_j - u_{j,h}^M\|_{0,\rho}^2 - 2\lambda_{j,h}^M b(u_j - \Pi_h^M u_j, u_{j,h}^M) \\ &\quad + 2a_h(u_j - \Pi_h^M u_j, \Pi_h^M u_j) + 2a_h(u_j - \Pi_h^M u_j, u_{j,h}^M - \Pi_h^M u_j). \end{aligned}$$

From Theorem 3.4, the first two terms can be bounded as

$$\|u_j - u_{j,h}^M\|_{0,\rho}^2 \lesssim |u_j - u_{j,h}^M|_{1,h}^2 \lesssim h^4.$$

From a standard interpolation theory in [26], the assumption $\|u_{j,h}^M\|_{0,\rho} = 1$, and Theorem 3.4 (b), the third and last terms have the estimates below

$$\begin{aligned} b(u_j - \Pi_h^M u_j, u_{j,h}^M) &\lesssim \|u_j - \Pi_h^M u_j\|_{0,\rho} \|u_{j,h}^M\|_{0,\rho} \lesssim h^3, \\ a_h(u_j - \Pi_h^M u_j, u_{j,h}^M - \Pi_h^M u_j) &\lesssim |u_j - \Pi_h^M u_j|_{1,h} |u_{j,h}^M - \Pi_h^M u_j|_{1,h} \lesssim h^4. \end{aligned}$$

When h is small enough, it follows from Lemma 3.2 that

$$a_h(u_j - \Pi_h^M u_j, \Pi_h^M u_j) \geq \alpha h^2.$$

Thus, $a_h(u_j - \Pi_h^M u_j, \Pi_h^M u_j)$ becomes the dominant term on the right-hand-side of (3.11). Hence the result. \square

4. REDUCED RECTANGULAR MORLEY ELEMENT SPACE FOR H^1 PROBLEMS

4.1. Reduced rectangular Morley element space. We introduce an reduced rectangular Morley (RRM) element space by

$$(4.1) \quad V_h^R := \left\{ w_h \in L^2(\Omega) : w_h|_K \in P_2(K), w_h(a) \text{ is continuous at any } a \in \mathcal{N}_h^i, \right. \\ \left. \text{and } \oint_e \partial_{n_e} w_h ds \text{ is continuous across any } e \in \mathcal{E}_h^i \right\},$$

and, associated with $H_0^1(\Omega)$, define

$$(4.2) \quad V_{hs}^R := \{ w_h \in V_h^R : w_h(a) = 0, \forall a \in \mathcal{N}_h^b \}.$$

Theorem 4.1. *If \mathcal{G}_h is a $m \times n$ rectangular subdivision of Ω , then $\dim(V_{hs}^R) = mn + 1$.*

Detailed proof of Theorems 4.1 and an available set of basis functions of V_{hs}^R are put in Appendix B.

For any function v_h in the RRM element space, the number of continuity restrictions across internal edges is greater than $\dim(P_2(K))$, which makes it a nontrivial task to find out a set of basis functions of V_{hs}^R , and it is not even easy to tell if the space contains non-zero functions. Actually, the proof of Theorem 4.1 in Appendix B ensures that the RRM element space is non-zero. From the analysis therein, the supports of the basis functions in V_{hs}^R are not completely local, making it complicated to construct an interpolation operator from V to V_{hs}^R , which, however, plays a fundamental role in the approximation error analysis.

Remark 4.2. Since a non-convex domain which can be covered by a rectangular subdivision can be considered as a combination of several rectangular regions, a nontrivial RRM element space can still be expected on it.

4.2. Approximation property of the RRM element space. The main result of this subsection is the theorem below.

Theorem 4.3. *Given $u \in H_0^1(\Omega) \cap H^3(\Omega)$, we have*

$$\inf_{v_h \in V_{hs}^R} |u - v_h|_{1,h} \lesssim h^\alpha |u|_{1+\alpha, \Omega}, \quad \alpha = 1, 2.$$

We postpone the proof of Theorem 4.3 after some technical lemmas. Let $\underline{f} \in (\underline{H}_n^1(\Omega))'$. We firstly consider the regularity of the Stokes problem: Find $(\underline{u}, p) \in \underline{H}_n^1(\Omega) \times L_0^2(\Omega)$, such that

$$(4.3) \quad \begin{cases} (\nabla \underline{u}, \nabla \underline{v}) + (p, \operatorname{div} \underline{v}) = (\underline{f}, \underline{v}), & \forall \underline{v} \in \underline{H}_n^1(\Omega), \\ (q, \operatorname{div} \underline{u}) = 0, & \forall q \in L_0^2(\Omega). \end{cases}$$

Lemma 4.4. *Let Ω be a rectangle. If $\underline{f} \in \underline{L}^2(\Omega)$, then $(\underline{u}, p) \in \underline{H}^2(\Omega) \times H^1(\Omega)$.*

Proof. As $\text{div} \underline{u} = 0$, there exists a unique $\varphi \in H^2(\Omega) \cap H_0^1(\Omega)$, such that $\text{curl} \varphi = \underline{u}$. Moreover, φ solves the biharmonic equation:

$$(\nabla \text{curl} \varphi, \nabla \text{curl} \psi) = (\underline{f}, \text{curl} \psi), \quad \forall \psi \in H^2(\Omega) \cap H_0^1(\Omega).$$

By the regularity theory of the biharmonic equation (see [3, Theorem 2]), we have $\varphi \in H^3(\Omega)$,

and $\|\varphi\|_{3,\Omega} \lesssim \sup_{\psi \in H_0^1(\Omega) \setminus \{0\}} \frac{(\underline{f}, \text{curl} \psi)}{\|\psi\|_{1,\Omega}} \lesssim \|\underline{f}\|_{0,\Omega}$. Furthermore, $\nabla p = \underline{f} + \Delta \underline{u}$, and $\|p\|_{1,\Omega} \lesssim \|\underline{f} + \Delta \underline{u}\|_{0,\Omega} \lesssim \|\underline{f}\|_{0,\Omega}$. The proof is completed. \square

A related finite element problem is to find $(\underline{u}_h, q_h) \in \underline{V}_{hm}^{\text{BL}} \times \mathcal{L}_{h0}^0$, such that

$$(4.4) \quad \begin{cases} (\nabla \underline{u}_h, \nabla \underline{v}_h) + (p_h, \text{div} \underline{v}_h) &= (\underline{f}, \underline{v}_h) \\ (q_h, \text{div} \underline{u}_h) &= 0. \end{cases}$$

To ensure the convergence of the finite element scheme in Theorem 4.5, we need the following hypothesis:

Hypothesis RT. A rectangular grid \mathcal{G}_h is called to satisfy the hypothesis **Hypothesis RT** if and only if it is generated by refining a grid \mathcal{G}_{4h} twice.

Theorem 4.5. *Let \mathcal{G}_h be a grid that satisfies **Hypothesis RT**. Let (\underline{u}, p) and (\underline{u}_h, p_h) be the solutions of (4.3) and (4.4), respectively. If $(\underline{u}, p) \in \underline{H}^2(\Omega) \times H^1(\Omega)$, then*

$$(4.5) \quad |\underline{u} - \underline{u}_h|_{1,\Omega} \lesssim h(|u|_{2,\Omega} + |p|_{1,\Omega}),$$

and further

$$(4.6) \quad \|\underline{u} - \underline{u}_h\|_{0,\Omega} \lesssim h^2(|u|_{2,\Omega} + |p|_{1,\Omega}).$$

Based on Lemma 4.4, the proof of Theorem 4.5 is just a duplication of the proofs of [8, Theorems 3.4–3.5 and Corollary 3.2], and we omit the details here.

Theorem 4.6. *Let \mathcal{G}_h be a grid that satisfies **Hypothesis RT**. Given $\underline{w} \in \underline{H}_n^1(\Omega) \cap \underline{H}^2(\Omega)$ satisfying $\operatorname{div} \underline{w} = 0$. It holds that*

$$(4.7) \quad \inf_{\underline{w}_h \in \underline{V}_{hn}^{\text{PS}}, \operatorname{div}_h \underline{w}_h = 0} h|\underline{w} - \underline{w}_h|_{1,\Omega} + \|\underline{w} - \underline{w}_h\|_{0,\Omega} \lesssim h^2|\underline{w}|_{2,\Omega}.$$

Proof. Let \underline{u} be the exact velocity of (4.3). Denote $p_0 \equiv 0$. It can be verified directly that the pair $(\underline{u}, p_0 \equiv 0) \in \underline{H}_n^1(\Omega) \times L_0^2(\Omega)$ solves the equation

$$(4.8) \quad \begin{cases} (\nabla \underline{u}, \nabla \underline{v}) + (p_0, \operatorname{div} \underline{v}) &= (-\Delta \underline{u}, \underline{v}) \\ (q, \operatorname{div} \underline{u}) &= 0, \end{cases}$$

Let $(\underline{y}_h, p_{0h}) \in \underline{V}_{hn}^{\text{BL}} \times \mathcal{L}_{h0}^0$ solve

$$(4.9) \quad \begin{cases} (\nabla \underline{y}_h, \nabla \underline{v}_h) + (p_{0h}, \operatorname{div} \underline{v}_h) &= (-\Delta \underline{u}, \underline{v}_h) \\ (q_h, \operatorname{div} \underline{y}_h) &= 0, \end{cases}$$

then $h|\underline{w} - \underline{y}_h|_{1,\Omega} + \|\underline{w} - \underline{y}_h\|_{0,\Omega} \leq Ch^2|\underline{u}|_{2,\Omega}$. Set $\underline{w}_h := \underline{\Pi}_h^{\text{rQ}} \underline{y}_h$, then, from Lemma 2.4, $\underline{w}_h \in \underline{V}_{hn}^{\text{PS}}$.

Moreover, it is easy to verify that

$$(\operatorname{div}_h \underline{w}_h, q_h) = (\operatorname{div} \underline{y}_h, q_h) = 0, \quad \forall q_h \in \mathcal{L}_{h0}^0,$$

namely $\operatorname{div}_h \underline{w}_h = 0$. Furthermore,

$$|\underline{w} - \underline{w}_h|_{1,h} \leq |\underline{w} - \underline{\Pi}_h^{\text{rQ}} \underline{w}|_{1,\Omega} + |\underline{\Pi}_h^{\text{rQ}}(\underline{w} - \underline{y}_h)|_{1,h} \lesssim h|\underline{w}|_{2,\Omega},$$

and

$$\|\underline{w} - \underline{w}_h\|_{0,\Omega} = \|\underline{w} - \underline{y}_h + (\operatorname{Id} - \underline{\Pi}_h^{\text{rQ}})(\underline{y}_h - \underline{w}) + (\operatorname{Id} - \underline{\Pi}_h^{\text{rQ}})\underline{w}\|_{0,\Omega} \lesssim h^2|\underline{w}|_{2,\Omega}.$$

Hence the result. □

Lemma 4.7. *For the curl of space V_{hs}^{R} , it can be depicted as a special subspace of the vector Park–Sheen element space, i.e.,*

$$\operatorname{curl}_h V_{hs}^{\text{R}} = \{\underline{z}_h \in \underline{V}_{hn}^{\text{PS}} : \operatorname{div}_h \underline{z}_h = 0\}.$$

Proof. Firstly, by standard argument, we can prove the exact sequence which reads

$$(4.10) \quad 0 \longrightarrow V_{hs}^M \xrightarrow{\text{curl}_h} \underline{V}_{hm}^{\text{LTZ}} \xrightarrow{\text{div}_h} \mathcal{L}_h^{1,-1} \longrightarrow 0,$$

where $\mathcal{L}_h^{1,-1} = \{q \in L_0^2(\Omega) : q|_K \in P_1(K)\}$. This way, given $\underline{v}_h \in \underline{V}_{hm}^{\text{PS}} \subset \underline{V}_{hm}^{\text{LTZ}}$ with $\text{div}_h \underline{v}_h = 0$, there exists $w_h \in V_{hs}^M$, such that $\text{curl}_h w_h = \underline{v}_h$. Since \underline{v}_h is piecewise linear polynomial, w_h is piecewise quadratic, namely $w_h \in V_{hs}^R$. On the other hand, it is evident that $\text{curl}_h V_{hs}^R \subset \{\underline{z}_h \in \underline{V}_{hm}^{\text{PS}} : \text{div}_h \underline{z}_h = 0\}$.

Hence the result. \square

Proof of Theorem 4.3. By Theorem 4.6 and Lemma 4.7,

$$(4.11) \quad \inf_{v_h \in V_{hs}^R} |u - v_h|_{1,h} = \inf_{v_h \in V_{hs}^R} \|\text{curl}u - \text{curl}v_h\|_{0,\Omega} \\ = \inf_{\underline{w}_h \in \underline{V}_{hm}^{\text{PS}}, \text{div}_h \underline{w}_h = 0} \|\text{curl}u - \underline{w}_h\|_{0,h} \lesssim h^\alpha |\text{curl}u|_{\alpha,\Omega} \lesssim h^\alpha |u|_{1+\alpha,\Omega}, \quad \alpha = 1, 2.$$

The proof is completed. \square

5. CONVERGENCE ANALYSIS OF THE RRM ELEMENT SCHEMES

5.1. Optimal convergence for the source problem. For the RM element space V_{hs}^M and the RRM element space V_{hs}^R , the discrete source problems are given as:

Find $u_h^M \in V_{hs}^M$, such that

$$(5.1) \quad a_h(u_h^M, v_h) = b(f, v_h), \quad \forall v_h \in V_{hs}^M,$$

Find $u_h^R \in V_{hs}^R$, such that

$$(5.2) \quad a_h(u_h^R, v_h) = b(f, v_h), \quad \forall v_h \in V_{hs}^R.$$

It is obvious that $V_{hs}^R = V_{hs}^M \cap V_{h0}^W$, and we infer that the RRM element is a quadratic nonconforming element on rectangles with a second-order convergence rate in the energy norm. We will verify this assertion strictly in this section.

Theorem 5.1. *Let \mathcal{G}_h be a grid that satisfies Hypothesis RT. Let u and u_h^R be the solutions of (2.2) and (5.2), respectively. It holds that*

- (a) if $u \in H_0^1(\Omega) \cap H^2(\Omega)$, then $|u - u_h^R|_{1,h} \lesssim h|u|_{2,\Omega}$ and $\|u - u_h^R\|_{0,\rho} \lesssim h^2|u|_{2,\Omega}$;
- (b) if $u \in H_0^1(\Omega) \cap H^3(\Omega)$ and the mesh is uniform, then $|u - u_h^R|_{1,h} \lesssim h^2|u|_{3,\Omega}$.

Proof. (a) By the Strang lemma, we have

$$(5.3) \quad |u - u_h^R|_{1,h} \lesssim \inf_{v_h \in V_{hs}^R} |u - v_h|_{1,h} + \sup_{w_h \in V_{hs}^R, w_h \neq 0} \frac{E_h(u, w_h)}{|w_h|_{1,h}}.$$

For the first term in the right hand side of (5.3), we have from Theorem 4.3 that

$$(5.4) \quad \inf_{v_h \in V_{hs}^R} |u - v_h|_{1,h} \lesssim h|u|_{2,\Omega}.$$

For the second term, we have from Lemma 3.1 and $V_{hs}^R \subset V_{hs}^M$ that

$$(5.5) \quad |E_h(u, w_h)| \lesssim \sum_{K \in \mathcal{G}_h} h_K^2 |u|_{2,K} |w_h|_{2,K} \lesssim h|u|_{2,\Omega} |w_h|_{1,h}, \quad \forall w_h \in V_h^R.$$

Submit (5.4) and (5.5) into (5.3), and we obtain $|u - u_h^R|_{1,h} \lesssim h|u|_{2,\Omega}$, where $u \in H_0^1(\Omega) \cap H^2(\Omega)$.

Given $g \in Q$, let $\phi_g \in V$ and $\phi_{gh} \in V_{hs}^R$ be the solutions of the two problems below, respectively,

$$a(v, \phi_g) = b(g, v), \quad \forall v \in V; \quad a_h(v_h, \phi_{gh}) = b(g, v_h), \quad \forall v_h \in V_{hs}^R.$$

By the Nitsche-Lascaux-Lesaint lemma (see e.g., [26, Theorem 5.3.1]), it holds that

$$(5.6) \quad \|u - u_h^R\|_{0,\rho} \lesssim |u - u_h^R|_{1,h} \sup_{g \in Q, g \neq 0} \left\{ \frac{1}{\|g\|_{0,\rho}} |\phi_g - \phi_{gh}|_{1,h} \right\} + \sup_{g \in Q, g \neq 0} \left\{ \frac{1}{\|g\|_{0,\rho}} (E_h(\phi_g, u_h^R) + E_h(u, \phi_{gh})) \right\}.$$

For the first term in the right side of (5.6), we have

$$(5.7) \quad |u - u_h^R|_{1,h} \sup_{g \in Q, g \neq 0} \left\{ \frac{1}{\|g\|_{0,\rho}} |\phi_g - \phi_{gh}|_{1,h} \right\} \lesssim h|u|_{2,\Omega} \frac{h|\phi_g|_{2,\Omega}}{\|g\|_{0,\rho}} \lesssim h^2|u|_{2,\Omega} \frac{\|g\|_{0,\rho}}{\|g\|_{0,\rho}} \lesssim h^2|u|_{2,\Omega},$$

where we utilize the regularity of solution on a convex domain, namely, $|\phi_g|_{2,\Omega} \lesssim \|g\|_{0,\rho}$.

For the second term, we notice that

$$(5.8) \quad |E_h(\phi_g, u_h^R)| \lesssim \sum_{K \in \mathcal{G}_h} h_K^2 |\phi_g|_{2,K} |u_h^R|_{2,K} \lesssim h|\phi_g|_{2,\Omega} \left(\sum_{K \in \mathcal{G}_h} h_K^2 |u_h^R|_{2,K}^2 \right)^{1/2}.$$

Let $\Pi_{h0}^p : L^2(\Omega) \mapsto V_{hs}^M$ be an average projection operator defined in [26]. From [26, Theorem 3.5.4], we have $|u - \Pi_{h0}^p u|_{1,K} \lesssim h_K |u|_{2,K}$ and $|\Pi_{h0}^p u|_{2,K} \lesssim |u|_{2,K}$. Thus we obtain

$$(5.9) \quad \begin{aligned} \sum_{K \in \mathcal{G}_h} h_K^2 |u_h^R|_{2,K}^2 &\leq 2 \sum_{K \in \mathcal{G}_h} h_K^2 (|u_h^R - \Pi_{h0}^p u|_{2,K}^2 + |\Pi_{h0}^p u|_{2,K}^2) \lesssim \sum_{K \in \mathcal{G}_h} (|u_h^R - \Pi_{h0}^p u|_{1,K}^2 + h_K^2 |u|_{2,K}^2) \\ &\lesssim \sum_{K \in \mathcal{G}_h} (|u - u_h^R|_{1,K}^2 + |u - \Pi_{h0}^p u|_{1,K}^2 + h_K^2 |u|_{2,K}^2) \lesssim |u - u_h^R|_{1,h}^2 + h^2 |u|_{2,\Omega}^2 \lesssim h^2 |u|_{2,\Omega}^2. \end{aligned}$$

The last inequality holds due to the fact that $|u - u_h^R|_{1,h} \lesssim h|u|_{2,\Omega}$. Submitting (5.9) into (5.8), it yields

$$|E_h(\phi_g, u_h^R)| \lesssim h^2 |\phi_g|_{2,\Omega} |u|_{2,\Omega} \lesssim h^2 \|g\|_{0,\rho} |u|_{2,\Omega}. \quad \text{Similarly, it holds that } |E_h(u, \phi_{gh})| \lesssim h^2 |u|_{2,\Omega} \|g\|_{0,\rho}.$$

Thus we have

$$(5.10) \quad \sup_{g \in Q, g \neq 0} \left\{ \frac{1}{\|g\|_{0,\rho}} \left(E_h(u, \phi_{gh}) + E_h(\phi_g, u_h^R) \right) \right\} \lesssim h^2 |u|_{2,\Omega}.$$

Submit (5.7) and (5.10) into (5.6), and we obtain $\|u - u_h^R\|_{0,\rho} \lesssim h^2 |u|_{2,\Omega}$, where $u \in H_0^1(\Omega) \cap H^2(\Omega)$.

(b) If $u \in H_0^1(\Omega) \cap H^3(\Omega)$ and the mesh is uniform, then $\inf_{v_h \in V_{hs}^R} |u - v_h|_{1,h} \lesssim h^2 |u|_{3,\Omega}$. From Lemma 3.1,

$$|E_h(u, v_h)| \lesssim h^2 |u|_{3,\Omega} |v_h|_{1,h}, \quad \forall v_h \in V_h^R. \quad \text{Hence we have } |u - u_h|_{1,h} \lesssim h^2 |u|_{3,\Omega}. \quad \square$$

It shows that the error estimate in the energy norm can be $O(h^2)$ when the mesh is uniform. However, the convergence rate in L^2 -norm can not be improved on uniform grids. Actually, there exists a lower bound stated in the following Theorem 5.2.

Theorem 5.2. *Let \mathcal{G}_h be a uniform grid satisfying **Hypothesis RT**. Let u and u_h^R be the solutions of (2.2) and (5.2), respectively. If $\|f\|_{0,\rho} \neq 0$ and $u \in H_0^1(\Omega) \cap H^3(\Omega)$, then $\|u - u_h^R\|_{0,\rho} \gtrsim h^2$, provided that h is small enough.*

Proof. Let u_h^M be the solution of (5.1). Then

$$(5.11) \quad b(-f, u - u_h^M) \geq \delta h^2,$$

given that h is small enough, where $\delta > 0$ is a constant independent of h ; see [22, Lemma 3.18].

Noticing that $V_{hs}^R \subset V_{hs}^M$, we obtain

$$(5.12) \quad a_h(u_h^M - u_h^R, v_h) = 0, \quad \forall v_h \in V_{hs}^R.$$

A simple division yields

$$(5.13) \quad b(-f, u - u_h^R) = b(-f, u - u_h^M) + b(-f, u_h^M - u_h^R).$$

Owing to the orthogonality and $|u_h^M - u_h^R|_{1,h} \leq |u_h^M - u|_{1,h} + |u - u_h^R|_{1,h} \lesssim h^2$, it holds that

$$(5.14) \quad b(-f, u_h^M - u_h^R) = -a_h(u_h^M, u_h^M - u_h^R) = -a_h(u_h^M - u_h^R, u_h^M - u_h^R) = -|u_h^M - u_h^R|_{1,h}^2 \lesssim h^4.$$

A combination of (5.11), (5.13) and (5.14) leads to the following lower bound, provided that h is small enough,

$$b(-f, u - u_h^R) \geq \gamma h^2,$$

where $\gamma > 0$ is a constant independent of h . Therefore we have

$$\|u - u_h^R\|_{0,\rho} = \sup_{g \in Q, g \neq 0} \frac{b(g, u - u_h^R)}{\|g\|_{0,\rho}} \geq \frac{b(-f, u - u_h^R)}{\| -f \|_{0,\rho}} \geq \frac{\gamma}{\|f\|_{0,\rho}} h^2.$$

Hence the result. \square

Remark 5.3. [22, Remark 3.16] For rectangle domain, the condition $\|f\|_{0,\rho} \neq 0$ implies that $\left\|\frac{\partial^2 u}{\partial x \partial y}\right\|_{0,\rho} \neq 0$. In fact, if $\left\|\frac{\partial^2 u}{\partial x \partial y}\right\|_{0,\rho} = 0$, then u is of the form $u = h(x) + g(y)$, for some function $h(x)$ with respect to x and $g(y)$ with respect to y . Then, the boundary condition, i.e., $u = 0$ on $\partial\Omega$, indicates $u \equiv 0$, which contradicts $\|f\|_{0,\rho} \neq 0$.

5.2. Analysis of the scheme for the eigenvalue problem. With the associated spaces V_{hs}^M and V_{hs}^R , the discrete eigenvalue problems are given as:

Find $(\lambda_h^M, u_h^M) \in \mathbb{R} \times V_{hs}^M$ with $\|u_h^M\|_{0,\rho} = 1$, such that

$$(5.15) \quad a_h(u_h^M, v_h) = \lambda_h^M b(u_h^M, v_h), \quad \forall v_h \in V_{hs}^M,$$

Find $(\lambda_h^R, u_h^R) \in \mathbb{R} \times V_{hs}^R$ with $\|u_h^R\|_{0,\rho} = 1$, such that

$$(5.16) \quad a_h(u_h^R, v_h) = \lambda_h^R b(u_h^R, v_h), \quad \forall v_h \in V_{hs}^R.$$

From Theorem 5.4, the convergence results of the eigenvalue problem is obtained by standard argument (see, e.g., [9, 31, 32, 34]).

Theorem 5.4. Let \mathcal{G}_h be a grid satisfying **Hypothesis RT**. Let λ_j be the j -th eigenvalue of (2.4), and $(\lambda_{j,h}^R, u_{j,h}^R) \in \mathbb{R} \times V_{hs}^R$ be the j -th eigen-pair of (5.16) with $\|u_{j,h}^R\|_{0,\rho} = 1$. It holds that

(a) if $M(\lambda_j) \subset H_0^1(\Omega) \cap H^2(\Omega)$, then there exists $u_j \in M(\lambda_j)$ with $\|u_j\|_{0,\rho} = 1$, such that

$$|\lambda_j - \lambda_{j,h}^R| \lesssim h^2, \quad \|u_j - u_{j,h}^R\|_{0,\rho} \lesssim h^2, \quad \text{and} \quad |u_j - u_{j,h}^R|_{1,h} \lesssim h;$$

(b) if the mesh is uniform and $M(\lambda_j) \subset H_0^1(\Omega) \cap H^3(\Omega)$, then there exists $u_j \in M(\lambda_j)$ with $\|u_j\|_{0,\rho} = 1$, such that $|u_j - u_{j,h}^R|_{1,h} \lesssim h^2$.

Similar to the basic relation between V and its conforming approximation V_h^C for eigenvalue problems in [2], the following relation holds.

Lemma 5.5. Let (λ_h^M, u_h^M) be an eigen-pair of (5.15) with $\|u_h^M\|_{0,\rho} = 1$. Denote, the Rayleigh quotient, by $R(v_h) := \frac{a_h(v_h, v_h)}{b(v_h, v_h)}$. For any $v_h \in V_{hs}^M$ with $\|v_h\|_{0,\rho} = 1$, it holds that

$$(5.17) \quad R(v_h) - \lambda_h^M = |v_h - u_h^M|_{1,h}^2 - \lambda_h^M \|v_h - u_h^M\|_{0,\rho}^2.$$

Proof. From $\|v_h\|_{0,\rho} = \|u_h^M\|_{0,\rho} = 1$ and $\lambda_h^M = a_h(u_h^M, u_h^M)$, it is equivalent to prove that

$$\begin{aligned}
a_h(v_h, v_h) - a_h(u_h^M, u_h^M) &= a_h(v_h + u_h^M, v_h - u_h^M) \\
&= a_h(v_h - u_h^M, v_h - u_h^M) + 2a_h(u_h^M, v_h - u_h^M) \\
&= |v_h - u_h^M|_{1,h}^2 + 2\lambda_h^M b(u_h^M, v_h - u_h^M) \\
&= |v_h - u_h^M|_{1,h}^2 - \lambda_h^M [-2b(u_h^M, v_h) + b(u_h^M, u_h^M) + b(v_h, v_h)] \\
&= |v_h - u_h^M|_{1,h}^2 - \lambda_h^M b(v_h - u_h^M, v_h - u_h^M) \\
&= |v_h - u_h^M|_{1,h}^2 - \lambda_h^M \|v_h - u_h^M\|_{0,\rho}^2,
\end{aligned}$$

where we utilize again the assumption: $b(v_h, v_h) = b(u_h^M, u_h^M)$. \square

Theorem 5.6. *Let (λ_j, u_j) , $(\lambda_{j,h}^R, u_{j,h}^R)$ and $(\lambda_{j,h}^M, u_{j,h}^M)$ be the j -th exact eigen-pair and its discrete approximations with $\|u_j\|_{0,\rho} = \|u_{j,h}^R\|_{0,\rho} = \|u_{j,h}^M\|_{0,\rho} = 1$. Assume that $u_j \in H_0^1(\Omega) \cap H^3(\Omega)$ and the mesh is uniform. Provided that h is small enough, we have*

$$(5.18) \quad C_R h^2 \leq \lambda_j - \lambda_{j,h}^R \leq \lambda_j - \lambda_{j,h}^M,$$

where C_R is a positive constant independent of h .

Proof. Since $V_{hs}^R \subset V_{hs}^M$, the second inequality, or $\lambda_{j,h}^R \geq \lambda_{j,h}^M$, holds from the minimum-maximum principle [2]. Let $v_h = u_{j,h}^R$ in Lemma 5.5. We obtain

$$(5.19) \quad \lambda_{j,h}^R - \lambda_{j,h}^M = R(u_{j,h}^R) - \lambda_{j,h}^M = |u_{j,h}^R - u_{j,h}^M|_{1,h}^2 - \lambda_{j,h}^M \|u_{j,h}^R - u_{j,h}^M\|_{0,\rho}^2.$$

From Theorem 3.4, Theorem 5.4, and the triangle inequality, it holds that

$$(5.20) \quad |u_{j,h}^R - u_{j,h}^M|_{1,h}^2 - \lambda_{j,h}^M \|u_{j,h}^R - u_{j,h}^M\|_{0,\rho}^2 \lesssim h^4.$$

A combination of (3.10), (5.19), and (5.20) yields that

$$\lambda_j - \lambda_{j,h}^R = \lambda_j - \lambda_{j,h}^M + \lambda_{j,h}^M - \lambda_{j,h}^R \geq \alpha h^2 + o(h^2).$$

Hence the result. \square

Remark 5.7. To the best of our knowledge, the RM element and the RRM element are the only two elements, by which eigenvalue approximations have the same convergence rates as that of eigenfunction approximations in the energy norm.

5.3. Implementation and numerical results.

5.3.1. *Implementation.* Since constructing clearly a basis functions of V_{hs}^R on an arbitrary grid is sophisticated, we now present an available approach how (5.2) and (5.16) can be implemented. We start with the fact that $V_{hs}^R = \{w_h \in V_{h0}^W : \int_e \llbracket \partial_{n_e} w_h \rrbracket = 0, \forall e \in \mathcal{E}_h^i\}$. Define $P_0(\mathcal{E}_h^i)$ the space of piecewise constant functions defined on \mathcal{E}_h^i .

An equivalent formulation of (5.2) is to find $(u_h, \delta_h) \in V_{h0}^W \times P_0(\mathcal{E}_h^i)$, such that

$$(5.21) \quad \begin{cases} a_h(u_h, v_h) + \sum_{e \in \mathcal{E}_h^i} \int_e \llbracket \partial_{n_e} v_h \rrbracket \delta_h = b(f, v_h), \\ \sum_{e \in \mathcal{E}_h^i} \int_e \llbracket \partial_{n_e} u_h \rrbracket \mu_h = 0. \end{cases}$$

An equivalent formulation of (5.16) is to find $(\lambda_h, u_h, \delta_h) \in \mathbb{R} \times V_{h0}^W \times P_0(\mathcal{E}_h^i)$ with $\|u_h\|_{0,\rho} = 1$, such that

$$(5.22) \quad \begin{cases} a_h(u_h, v_h) + \sum_{e \in \mathcal{E}_h^i} \int_e \llbracket \partial_{n_e} v_h \rrbracket \delta_h = \lambda_h b(u_h, v_h), \\ \sum_{e \in \mathcal{E}_h^i} \int_e \llbracket \partial_{n_e} u_h \rrbracket \mu_h = 0. \end{cases}$$

Problem (5.21) admits a solution (u_h, δ_h) , where u_h solves problem (5.2), and problem (5.22) admits a solution $(\lambda_h, u_h, \delta_h)$, where (λ_h, u_h) solves problem (5.16).

Remark 5.8. It's worth mentioning that formulations (5.21) and (5.22) can be applied to an arbitrary quadrilateral grid [36]. For the case wherein the grid comprises rectangles, a detailed construction process of basis functions of V_{hs}^R is given in Appendix B, based on which (5.2) and (5.16) can be implemented directly in elliptic formulation.

5.3.2. *Numerical experiments.* Let $\Omega = (0, 1)^2$. We consider nonuniform meshes (see Figure 1) with $\frac{h_{x,K}}{h_{y,K}} \in \left\{ \frac{0.35}{0.65}, \frac{0.65}{0.35}, 1 \right\}$, and uniform meshes with $\frac{h_{x,K}}{h_{y,K}} = \frac{1}{2}$. Numerical examples of the source problem and the eigenvalue problem are given below.

Example 1 for the source problem.

Consider (2.1) with $f = 2\pi^2 \sin(\pi x) \sin(\pi y)$. The exact solution u is computed as $u = \sin(\pi x) \sin(\pi y)$. Apply (5.21) to get the discrete solutions on uniform and nonuniform meshes. From Figure 2, the convergence rate is $O(h)$ in the energy norm, and $O(h^2)$ in L^2 -norm, on a nonuniform mesh. Both rates reach $O(h^2)$ order on uniform grids.

Example 2 for the eigenvalue problem.

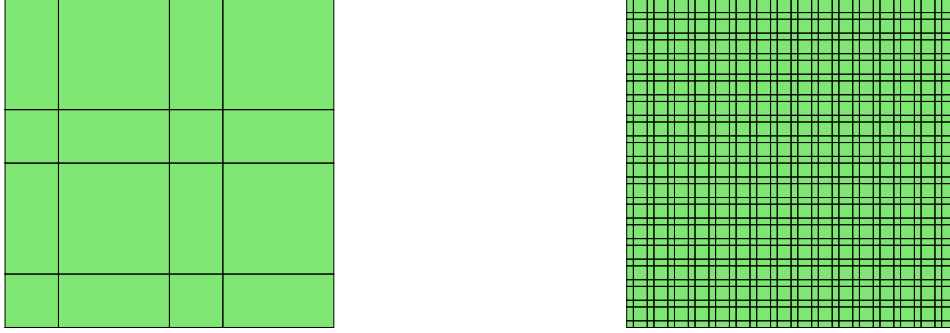


FIGURE 1. Illustration of a nonuniform shape regular subdivision. The partition in the right is a combination of small patterns as the left one.

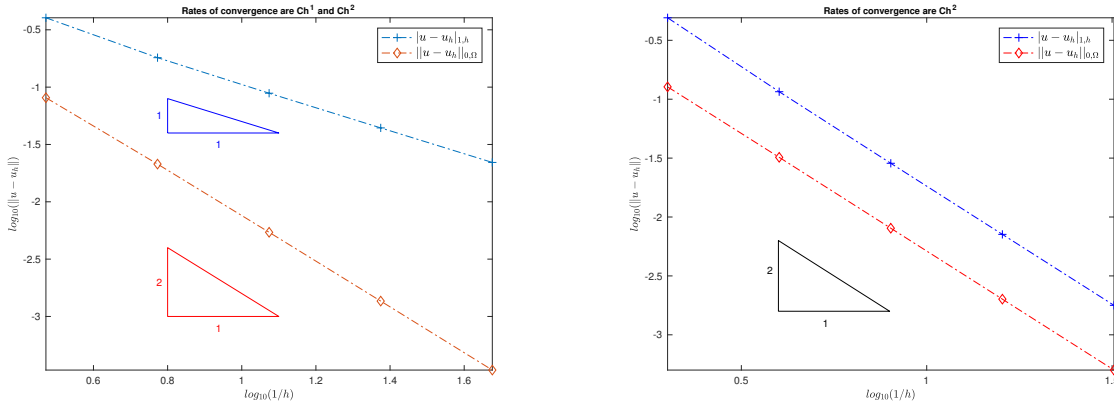


FIGURE 2. Source problem on rectangle domain: Errors in the energy norm and L^2 -norm with nonuniform (Left) or uniform (Right) subdivisions.

Consider (2.3) with $\rho = 1$. Then we have the exact eigenfunctions $u_{k,l} = 2\sin(k\pi x)\sin(l\pi y)$ and eigenvalues $\lambda_{k,l} = (k^2 + l^2)\pi^2$ ($k, l \in \mathbb{N}^+$). Arrange them by increasing order. Apply (5.22) to get the the smallest six discrete eigenvalues. From Figure 3, the convergence rates of eigenvalues almost reach $O(h^2)$ order in both nonuniform and uniform cases. Moreover, from tables 1 and 2, the eigenvalue approximations by the RRM element converge monotonically from below to the exact ones.

6. CONCLUSIONS AND DISCUSSIONS

6.1. Concluding remarks. In this paper, we present a reduced rectangular Morley element scheme for H^1 problems. Technically, the exactness relation between the RRM element and the PS element is figured out, and the approximation error estimate is established by an auxiliary Stokes problem. For the source problem, the convergence rate of this scheme is $O(h)$ in the energy norm and $O(h^2)$ in L^2 -norm, on general meshes. The error estimate in the energy norm reaches $O(h^2)$

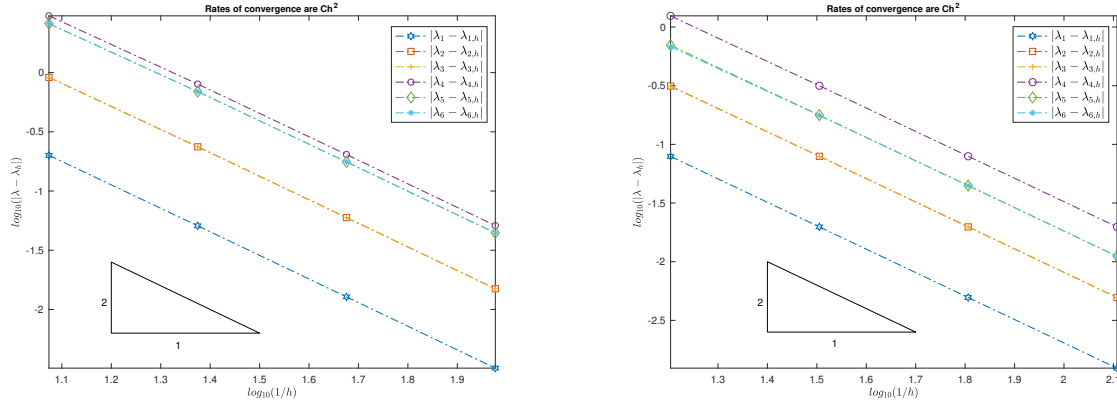


FIGURE 3. Eigenvalue problem on rectangle domain: Errors of eigenvalues with nonuniform subdivisions (Left) and uniform subdivisions (Right).

TABLE 1. Eigenvalues computed by the RRM element on nonuniform grids.

| h | $\lambda_{1,h}$ | order | $\lambda_{2,h}$ | $\lambda_{3,h}$ | order | $\lambda_{4,h}$ | order | $\lambda_{5,h}$ | $\lambda_{6,h}$ | order |
|-------------------|-----------------|-------|-----------------|-----------------|--------------|-----------------|-------|-----------------|-----------------|--------------|
| 0.3375 | 17.178 | | 38.419 | 39.047 | | 47.604 | | 65.324 | 78.711 | |
| 0.1688 | 18.982 | 1.690 | 46.125 | 46.126 | 1.696, 1.599 | 68.932 | 1.564 | 90.210 | 90.236 | 1.966, 1.181 |
| 0.084375 | 19.539 | 1.892 | 48.437 | 48.437 | 1.768, 1.768 | 75.941 | 1.662 | 96.105 | 96.106 | 1.638, 1.633 |
| 0.0421875 | 19.688 | 1.969 | 49.112 | 49.112 | 1.928, 1.928 | 78.157 | 1.884 | 98.004 | 98.004 | 1.873, 1.873 |
| 0.02109375 | 19.726 | 1.992 | 49.288 | 49.288 | 1.980, 1.980 | 78.754 | 1.968 | 98.520 | 98.520 | 1.964, 1.964 |
| 0.010546875 | 19.736 | 1.998 | 49.333 | 49.333 | 1.995, 1.995 | 78.906 | 1.992 | 98.652 | 98.652 | 1.991, 1.991 |
| Trend | ↗ | | ↗ | ↗ | | ↗ | | ↗ | ↗ | |
| Exact λ_j | 19.739 | – | 49.348 | 49.348 | | 78.957 | | 98.696 | 98.696 | |

TABLE 2. Eigenvalues computed by the RRM element on uniform grids.

| $h (= h_x)$ | $\lambda_{1,h}$ | order | $\lambda_{2,h}$ | $\lambda_{3,h}$ | order | $\lambda_{4,h}$ | order | $\lambda_{5,h}$ | $\lambda_{6,h}$ | order |
|-------------------|-----------------|-------|-----------------|-----------------|--------------|-----------------|-------|-----------------|-----------------|--------------|
| 0.25 | 18.559 | | 44.961 | 45.655 | | 63.427 | | 90.249 | 95.913 | |
| 0.125 | 19.428 | 1.896 | 48.127 | 48.163 | 1.796, 1.558 | 74.233 | 1.644 | 96.050 | 96.427 | 1.596, 0.613 |
| 0.0625 | 19.660 | 1.973 | 49.034 | 49.036 | 1.944, 1.899 | 77.711 | 1.896 | 97.996 | 98.016 | 1.890, 1.670 |
| 0.03125 | 19.719 | 1.993 | 49.269 | 49.269 | 1.986, 1.975 | 78.641 | 1.973 | 98.519 | 98.520 | 1.972, 1.928 |
| 0.015625 | 19.734 | 1.998 | 49.328 | 49.328 | 1.996, 1.994 | 78.878 | 1.993 | 98.652 | 98.652 | 1.993, 1.983 |
| 0.0078125 | 19.738 | 2.000 | 49.343 | 49.343 | 2.000, 1.996 | 78.937 | 1.998 | 98.685 | 98.685 | 1.998, 1.996 |
| Trend | ↗ | | ↗ | ↗ | | ↗ | | ↗ | ↗ | |
| Exact λ_j | 19.739 | | 49.348 | 49.348 | | 78.957 | | 98.696 | 98.696 | |

order on uniform grids. Besides, a lower bound of the L^2 -norm error is proved, and the best L^2 -norm error estimate is at most $O(h^2)$. For the eigenvalue problem, the discrete eigenvalues by the RM element and the RRM element are both proved to be lower bounds of the exact ones. In fact, the inequality (3.1), reads $a_h(w - \Pi_h^M w, \Pi_h^M w) \geq \alpha h^2$, or (3.2), reads $a_h(w - \Pi_h^M w, w) \geq \alpha_1 h^2$, is the dominant factor for the RRM element to yield these lower bounds, where Π_h^M is the interpolation operator for the RM element.

Roughly speaking, for schemes which provide the lower bounds of the eigenvalues, a smaller space provides a better approximation. This can be viewed as a motivation for the optimal space.

6.2. Further discussions. In this paper, we mainly focus on the convex domain (rectangle domain) case. Also, for the eigenvalue problem, we pay special attention to the computation of eigenvalues. Some more numerical experiments illustrate that the schemes can perform even better than the theoretical description in this paper. These can stimulate further research, and we list part of them below.

(1) Consider the eigenvalue problem (2.3) with $\rho = 1$ on $\Omega = (0, 1)^2$. From Figure 4, right, the convergence rate of the first eigenfunction in L^2 -norm reaches $O(h^3)$ order on uniform grids, while in Theorem 5.4 we can only derive $\|u_j - u_{j,h}^R\|_{0,\rho} \leq |u_j - u_{j,h}^R|_{1,h} \lesssim h^2$. Although, there exists a lower bound of the L^2 -norm error for the source problem, it may not hold for the eigenvalue problem, and it is possible that the convergence rate of the eigenfunctions in L^2 -norm may be higher than that in the energy norm.

(2) Consider the source problem (2.1) on L-shape domain: $\Omega = (0, 2)^2 \setminus [1, 2]^2$. From Figure 5, the convergence rates are consistent with the results derived on $\Omega = (0, 1)^2$. Although Theorem 5.1 for the source problem is based on the assumption of convex domain, this example implies that the RRM element may also be applicable to non-convex regions.

(3) Consider the eigenvalue problem (2.3) with $\rho = 1$ on L-shape domain. The eigenfunctions and eigenvalues are unknown, and eigenfunctions may have singularities around the reentrant corner. From [2], the third eigenfunction is analytic: $u_3 = \sin(\pi x)\sin(\pi x)$. We present the errors of u_3 in Figure 6, and observe that the convergence rates for error on L-shape domain are the same as that on a rectangle region. Moreover, the third eigenvalue computed by the RRM scheme satisfies $\lambda_{3,h} \leq \lambda_3 = 2\pi^2$ and the convergence rate is $O(h^2)$. The performance of the smallest six eigenvalues with nonuniform and uniform subdivisions are listed in Tables 3 and 4. These examples suggest

TABLE 3. Eigenvalues computed on L-shape domain with nonuniform subdivisions.

| h | $\lambda_{1,h}$ | $\lambda_{2,h}$ | $\lambda_{3,h}$ | order | $\lambda_{4,h}$ | $\lambda_{5,h}$ | $\lambda_{6,h}$ |
|---------------------|-----------------|-----------------|-----------------|-------|-----------------|-----------------|-----------------|
| 0.675 | 8.999 | 11.157 | 11.961 | | 16.776 | 17.955 | 23.829 |
| 0.3375 | 9.637 | 13.948 | 17.219 | 1.626 | 25.337 | 27.892 | 36.616 |
| 0.16875 | 9.708 | 14.840 | 18.984 | 1.739 | 28.190 | 30.865 | 40.131 |
| 0.084375 | 9.691 | 15.104 | 19.539 | 1.916 | 29.160 | 31.713 | 41.140 |
| 0.0421875 | 9.667 | 15.174 | 19.688 | 1.977 | 29.429 | 31.897 | 41.412 |
| 0.02109375 | 9.652 | 15.191 | 19.726 | 1.994 | 29.498 | 31.923 | 41.469 |
| 0.010546875 | 9.645 | 15.196 | 19.736 | 1.999 | 29.516 | 31.921 | 41.477 |
| Trend | | \nearrow | \nearrow | | \nearrow | | |
| $\lambda_j \approx$ | 9.640 | 15.197 | 19.739 | | 29.522 | 31.913 | 41.475 |

TABLE 4. Eigenvalues computed on L-shape domain with uniform subdivisions.

| $h_x = 2h_y$ | $\lambda_{1,h}$ | $\lambda_{2,h}$ | $\lambda_{3,h}$ | order | $\lambda_{4,h}$ | $\lambda_{5,h}$ | $\lambda_{6,h}$ |
|---------------------|-----------------|-----------------|-----------------|-------|-----------------|-----------------|-----------------|
| 0.5 | 9.894 | 13.443 | 15.857 | | 23.914 | 26.659 | 33.739 |
| 0.25 | 9.811 | 14.696 | 18.558 | 1.717 | 27.656 | 30.410 | 40.808 |
| 0.125 | 9.743 | 15.068 | 19.428 | 1.923 | 29.015 | 31.687 | 41.262 |
| 0.0625 | 9.691 | 15.165 | 19.660 | 1.980 | 29.392 | 31.921 | 41.456 |
| 0.03125 | 9.663 | 15.189 | 19.719 | 1.995 | 29.489 | 31.941 | 41.488 |
| 0.015625 | 9.650 | 15.195 | 19.734 | 1.999 | 29.513 | 31.930 | 41.485 |
| Trend | | \nearrow | \nearrow | | \nearrow | | |
| $\lambda_j \approx$ | 9.640 | 15.197 | 19.739 | | 29.522 | 31.913 | 41.475 |

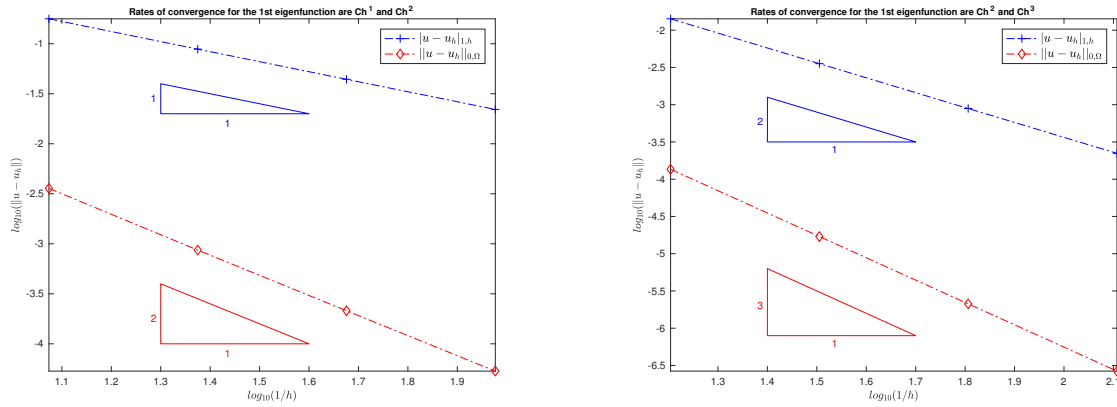
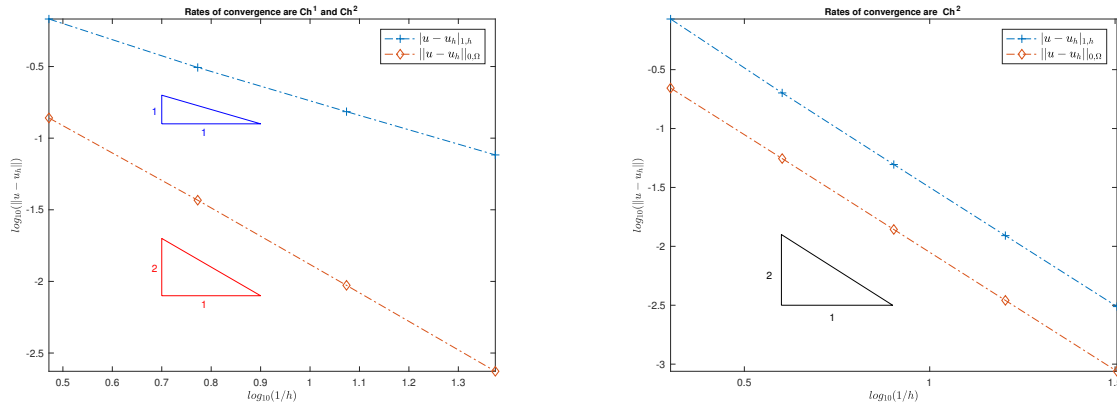


FIGURE 4. Eigenvalue problem on rectangle domain: Convergence rates of the 1st eigenfunction with nonuniform (Left) and uniform subdivisions (Right).

FIGURE 5. Source problem on L-shape domain: Errors in the energy norm and L^2 -norm with nonuniform (Left) and uniform subdivisions (Right).

that the RRM element may have better numerical applications, and these will be studied in our future work.

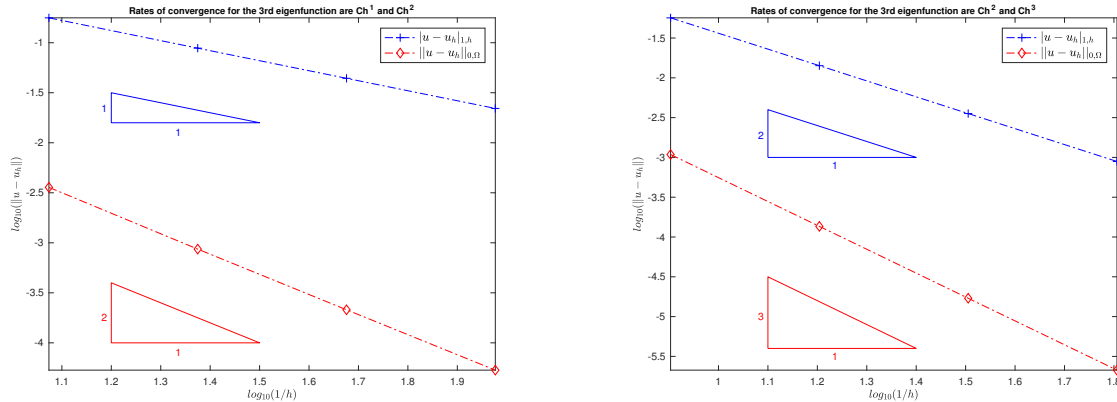


FIGURE 6. Eigenvalue problem on L-shape domain: Convergence rates of the 3rd eigenfunction with nonuniform (Left) and uniform subdivisions (Right).

REFERENCES

- [1] M. G. Armentano and R. G. Durán. Asymptotic lower bounds for eigenvalues by nonconforming finite element methods. *Electronic Transactions on Numerical Analysis*, 17(2):93–101, 2004.
- [2] I. Babuška and J. Osborn. Eigenvalue problems. In *Finite Element Methods (Part I)*, volume 2 of *Handbook of Numerical Analysis*, pages 641–787. Elsevier, 1991.
- [3] H. Blum, R. Rannacher, and R. Leis. On the boundary value problem of the biharmonic operator on domains with angular corners. *Mathematical Methods in the Applied Sciences*, 2(4):556–581, 1980.
- [4] C. Carstensen and D. Gallistl. Guaranteed lower eigenvalue bounds for the biharmonic equation. *Numerische Mathematik*, 126(1):33–51, 2014.
- [5] C. Carstensen and J. Gedicke. Guaranteed lower bounds for eigenvalues. *Mathematics of Computation*, 83(290):2605–2629, 2014.
- [6] C. Chen. *Finite element superconvergence structure theory*. Hunan Science and Technology Press, Hunan, 2001.
- [7] M. Fortin and M. Soulie. A non-conforming piecewise quadratic finite element on triangles. *International Journal for Numerical Methods in Engineering*, 19(4):505–520, 1983.
- [8] V. Girault and P. A. Raviart. *Finite element methods for Navier-Stokes equations: theory and algorithms*, volume 5. Springer Science & Business Media, 2012.
- [9] J. Hu, Y. Huang, and Q. Lin. Lower bounds for eigenvalues of elliptic operators: by nonconforming finite element methods. *Journal of Scientific Computing*, 61(1):196–221, 2014.
- [10] J. Hu and Z. Shi. The best L^2 norm error estimate of lower order finite element methods for the fourth order problem. *Journal of Computational Mathematics*, 30(5):449–460, 2012.
- [11] J. Hu and Z. Shi. A lower bound of the L^2 norm error estimate for the Adini element of the biharmonic equation. *Siam Journal on Numerical Analysis*, 51(5):2651–2659, 2013.
- [12] J. Hu, X. Yang, and S. Zhang. Capacity of the Adini element for biharmonic equations. *Journal of Scientific Computing*, 69(3):1366–1383, 2016.
- [13] J. Hu and S. Zhang. Nonconforming finite element methods on quadrilateral meshes. *Science China Mathematics*, 56(12):2599–2614, 2013.

- [14] J. Hu and S. Zhang. The minimal conforming H^k finite element spaces on \mathbb{R}^n rectangular grids. *Mathematics of Computation*, 84(292):563–579, 2015.
- [15] I. Kim, Z. Luo, Z. Meng, H. Nam, C. Park, and D. Sheen. A piecewise P_2 -nonconforming quadrilateral finite element. *ESAIM: Mathematical Modelling and Numerical Analysis*, 47(3):689–715, 2013.
- [16] H. Lee and D. Sheen. A new quadratic nonconforming finite element on rectangles. *Numerical Methods for Partial Differential Equations*, 22(4):954–970, 2006.
- [17] Y. Li. The lower bounds of eigenvalues by the Wilson element in any dimension. *Advances in Applied Mathematics and Mechanics*, 3(5):598–610, 2011.
- [18] Q. Lin and J. Lin. *Finite Element Methods: Accuracy and Improvement*. Science Press, Beijing, 2006.
- [19] Q. Lin, L. Tobiska, and A. Zhou. Superconvergence and extrapolation of non-conforming low order finite elements applied to the Poisson equation. *IMA Journal of Numerical Analysis*, 25(1):160–181, 2005.
- [20] Q. Lin, H. Xie, and J. Xu. Lower bounds of the discretization error for piecewise polynomials. *Mathematics of Computation*, 83(285):1–13, 2014.
- [21] F. Luo, Q. Lin, and H. Xie. Computing the lower and upper bounds of Laplace eigenvalue problem: by combining conforming and nonconforming finite element methods. *Science China Mathematics*, 55(5):1069–1082, 2012.
- [22] X. Meng, X. Yang, and S. Zhang. Convergence analysis of the rectangular Morley element scheme for second order problem in arbitrary dimensions. *Science China Mathematics*, 59(11):2245–2264, 2016.
- [23] C. Park and D. Sheen. P_1 -nonconforming quadrilateral finite element methods for second-order elliptic problems. *SIAM Journal on Numerical Analysis*, 41(2):624–640, 2003.
- [24] R. Rannacher and S. Turek. Simple nonconforming quadrilateral Stokes element. *Numerical Methods for Partial Differential Equations*, 8(2):97–111, 1992.
- [25] Z. Shi. A remark on the optimal order of convergence of Wilson’s nonconforming element. *Mathematica Numerica Sinica*, 8(2):159–163, 1986.
- [26] Z. Shi and M. Wang. *Finite element methods*. Science Press, Beijing, 2013.
- [27] M. Wang and J. Xu. Minimal finite element spaces for $2m$ -th-order partial differential equations in \mathbb{R}^n . *Mathematics of Computation*, 82(281):25–43, 2012.
- [28] E. Wilson, R. Taylor, W. Doherty, and J. Ghaboussi. Incompatible displacement models. In *Numerical and Computer Methods in Structural Mechanics*, pages 43–57. Academic Press, New York, 1973.
- [29] S. Wu and J. Xu. Nonconforming finite element spaces for $2m$ -th order partial differential equations on \mathbb{R}^n simplicial grids when $m = n + 1$. *Mathematics of Computation*, 88(316):531–551, 2019.
- [30] J. Xu. Iterative methods by space decomposition and subspace correction. *SIAM Review*, 34(4):581–613, 1992.
- [31] J. Xu and A. Zhou. A two-grid discretization scheme for eigenvalue problems. *Mathematics of Computation*, 70(233):17–25, 2001.
- [32] Y. Yang and Z. Chen. The order-preserving convergence for spectral approximation of self-adjoint completely continuous operators. *Science in China Series A: Mathematics*, 51(7):1232–1242, 2008.
- [33] Y. Yang, J. Han, H. Bi, and Y. Yu. The lower/upper bound property of the Crouzeix–Raviart element eigenvalues on adaptive meshes. *Journal of Scientific Computing*, 62(1):284–299, 2015.
- [34] Y. Yang, Z. Zhang, and F. Lin. Eigenvalue approximation from below using non-conforming finite elements. *Science in China Series A: Mathematics*, 53(1):137–150, 2010.

- [35] S. Zhang. Stable finite element pair for Stokes problem and discrete stokes complex on quadrilateral grids. *Numerische Mathematik*, 133(2):371–408, 2016.
- [36] S. Zhang. Minimal consistent finite element space for the biharmonic equation on quadrilateral grids. *IMA Journal of Numerical Analysis*, 2019.
- [37] Z. Zhang, Y. Yang, and C. Zhen. Eigenvalue approximation from below by Wilson’s element. *Mathematica Numerica Sinica*, 29(3):319–321, 2007.

APPENDIX A. CONSTRUCTION OF BASIS FUNCTIONS FOR THE MOMENT-CONTINUOUS (MC) ELEMENT SPACE

Let $\Omega \subset \mathbb{R}^2$ be a polygonal region subdivided into a rectangular grid \mathcal{G}_h . Define the moment-continuous (MC) element spaces as

$$(A.1) \quad V_h^{\text{MC}} := \{w_h \in L^2(\Omega) : w_h|_K \in P_2(K), \text{ and } w_h \text{ is moment-continuous on } \mathcal{G}_h\};$$

$$(A.2) \quad V_{h0}^{\text{MC}} := \{w_h \in V_h^{\text{MC}} : w_h \text{ is moment-homogeneous on } \mathcal{G}_h\}.$$

They have the following equivalent definitions:

$$(A.3) \quad V_h^{\text{MC}} := \{w_h \in L^2(\Omega) : w_h|_K \in P_2(K), \text{ and } w_h \text{ is continuous at second Gauss–Legendre points of any } e \in \mathcal{E}_h\};$$

$$(A.4) \quad V_{h0}^{\text{MC}} := \{w_h \in V_h^{\text{MC}} : w_h \text{ vanishes at second Gauss–Legendre points on any } e \in \mathcal{E}_h^b\}.$$

In this section, we will present available sets of basis functions of V_h^{MC} and V_{h0}^{MC} .

A.1. Compatibility conditions. Let K be a rectangle with a_i the vertices and g_{ij} the Gauss–Legendre points on the boundary (see Figure 7), where $i = 1, 2, 3, 4$ and $j = 1, 2$. Let $\theta_1 = \frac{1}{2}(1 - \sqrt{\frac{1}{3}})$ and $\theta_2 = \frac{1}{2}(1 + \sqrt{\frac{1}{3}})$ be the coordinates of second-order Gauss-Legendre points on $[0, 1]$. By a pure linear algebra argument, we have the following description of $P_2(K)$.

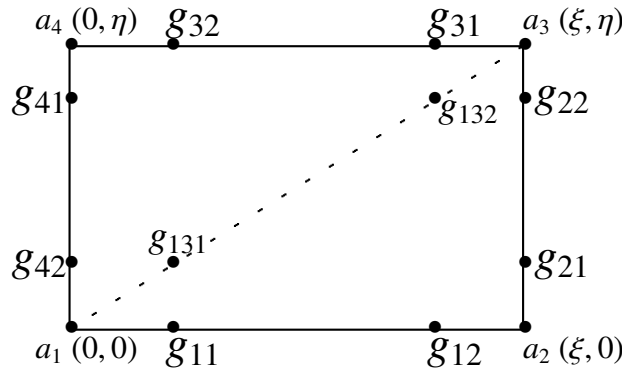


FIGURE 7. Illustration of Gauss points on the boundary of a rectangle.

Lemma A.1. *Given $\delta_{ij} \in \mathbb{R}$, $i = 1, 2, 3, 4$, $j = 1, 2$. There exists $p \in P_2(K)$, such that $p(g_{ij}) = \delta_{ij}$, if and only if the following compatibility conditions are satisfied on K ,*

$$(A.5) \quad \delta_{11} - \delta_{12} + \delta_{21} - \delta_{22} + \delta_{31} - \delta_{32} + \delta_{41} - \delta_{42} = 0;$$

$$(A.6) \quad \theta_1(\delta_{11} - \delta_{32}) + \theta_2(\delta_{31} - \delta_{12}) + (\delta_{21} - \delta_{22}) = 0;$$

$$(A.7) \quad \theta_1(\delta_{11} - \delta_{12}) + (\theta_2 - \theta_1)(\delta_{22} - \delta_{41}) + \theta_2(\delta_{32} - \delta_{31}) = 0.$$

Proof. To prove (A.5), we connect the vertices a_1 and a_3 . Let g_{131} and g_{132} be the two Gauss points on a_1a_3 . Then we obtain that (see [7, (2)])

$$p(g_{11}) - p(g_{12}) + p(g_{21}) - p(g_{22}) + p(g_{132}) - p(g_{131}) = 0$$

and

$$p(g_{31}) - p(g_{32}) + p(g_{41}) - p(g_{42}) + p(g_{131}) - p(g_{132}) = 0.$$

Thus (A.5) follows. Since the two directional derivatives of p belongs to $P_1(K)$, (A.6) and (A.7) hold. \square

A set of basis functions of $P_2(K)$ are listed below. Note that with φ_{a_i} being the bilinear functions and φ_{xx} and φ_{yy} being the bubbles in two directions, these six functions form a set of basis functions with respect to the Wilson element.

Local basis functions of $P_2(K)$:

$$(A.8) \quad \begin{cases} \varphi_{a_1, K} = \frac{1}{\xi\eta}(\xi - x)(\eta - y), \\ \varphi_{a_2, K} = \frac{1}{\xi\eta}x(\eta - y), \\ \varphi_{a_3, K} = \frac{1}{\xi\eta}xy, \\ \varphi_{a_4, K} = \frac{1}{\xi\eta}(\xi - x)y, \\ \varphi_{xx, K} = x(\xi - x), \\ \varphi_{yy, K} = y(\eta - y). \end{cases}$$

Lemma A.2. *Let $p \in P_2(K)$. The following results hold.*

- (1) *If $p(g_{41}) = p(g_{42}) = 0$, then $p \in \text{span}\{\varphi_{a_2}, \varphi_{a_3}, \varphi_{xx}, \varphi_{0, K}\}$;*
- (2) *If $p(g_{11}) = p(g_{12}) = p(g_{41}) = p(g_{42}) = 0$, then $p \in \text{span}\{\varphi_{a_3}, \varphi_{0, K}\}$;*
- (3) *If $p(g_{11}) = p(g_{12}) = p(g_{21}) = p(g_{22}) = p(g_{41}) = p(g_{42}) = 0$, then $p \in \text{span}\{\varphi_{0, K}\}$.*

Remark A.3. A polynomial $p \in P_2(K)$ is uniquely determined by its evaluations on g_{ij} only up to $\varphi_{0, K}(x, y) := \frac{1}{\xi^2}\varphi_{xx, K} + \frac{1}{\eta^2}\varphi_{yy, K} - 2\theta_1\theta_2$ multiplied by a constant.

A.2. Patterns of supports of basis functions in V_h^{MC} and V_{h0}^{MC} . Suppose that the domain is divided into $m \times n$ rectangles; see Figure 8. In x direction, it is decomposed to m rows, each being \mathcal{G}_i ($1 \leq i \leq m$), and in y direction, it is decomposed to n columns, each being \mathcal{G}^j ($1 \leq j \leq n$). The

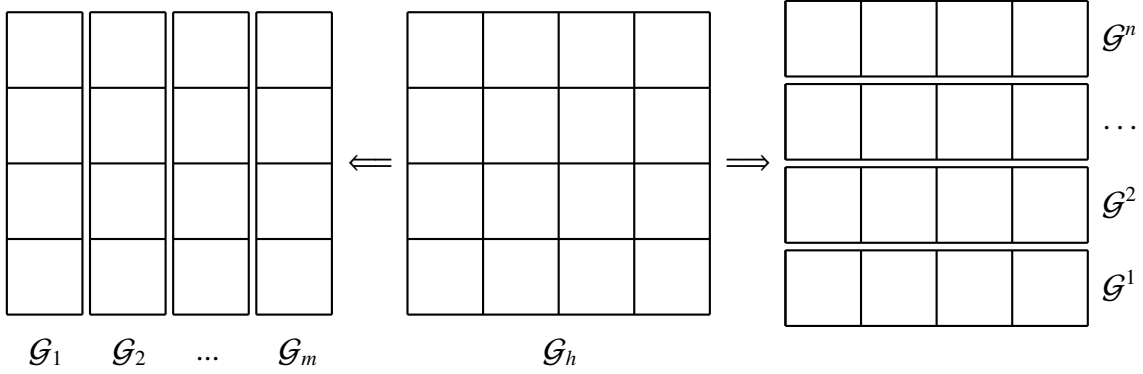


FIGURE 8. Illustration of the domain and the grid.

vertices are labeled by X_i^j , and the cells by K_i^j . That is, $K_i^j = \mathcal{G}_i \cap \mathcal{G}^j$, and it has four vertices as X_{i-1}^{j-1} , X_i^{j-1} , X_{i-1}^j , and X_i^j .

We call the support set of a basis function a pattern. Below we present four kinds of patterns sequentially, namely, cell patterns in Lemma A.4, vertex patterns in Lemma A.5, column patterns and row patterns in Lemma A.6.

Lemma A.4. *Let φ_{0,K_i^j} be defined in Remark A.3 on K_i^j , $1 \leq i \leq m$, $1 \leq j \leq n$. Then, $\varphi_{0,K_i^j} \in V_{h0}^{MC}$.*

Lemma A.5. *Let $\varphi_{X_i^j}$ denote a function defined on the support patch ω associated with X_i^j , which is bilinear on every element in ω . Then, $\varphi_{X_i^j} \in V_h^{MC}$, $\forall X_i^j \in \mathcal{N}_h$, and $\varphi_{X_i^j} \in V_{h0}^{MC}$, $\forall X_i^j \in \mathcal{N}_h^i$.*

Lemma A.6. *Let ω be a patch with boundaries Γ_l ($l = 1 : 4$), anticlockwise; see Figure 9. Let $V_h^{MC}(\omega)$ denote a moment-continuous space restricted on ω .*

(a) *Let $\omega = \mathcal{G}_i$ be the union of elements in the i -th column; see Figure 9 (Left). We define*

$$V_{\text{col},i}^{\text{MC}} := \left\{ v_h \in V_h^{\text{MC}}(\omega); v_h \text{ vanishes at all Gauss-Legendre points on } e \subset \Gamma_l \text{ (} l = 1, 3 \text{)} \right\}.$$

Let φ_i^x be a function defined on ω , which is equal to φ_{xx,K_i^j} on every $K_i^j \in \omega$. Then $\varphi_i^x \in V_{\text{col},i}^{\text{MC}}$, and furthermore, $V_{\text{col},i}^{\text{MC}} = \text{span}\{\varphi_i^x\} \oplus \text{span}\{\varphi_{0,K_i^j}\}_{j=1}^n$.

(b) *Let $\omega := \mathcal{G}^j$ be the union of elements in the j -th row; see Figure 9 (Right). We define*

$$V_{\text{row},j}^{\text{MC}} := \left\{ v_h \in V_h^{\text{MC}}(\omega); v_h \text{ vanishes at all Gauss-Legendre points on } e \subset \Gamma_l \text{ (} l = 2, 4 \text{)} \right\}$$

Let φ_j^y be a function defined on ω , which is equal to φ_{yy,K_i^j} on every $K_i^j \in \omega$. Then $\varphi_j^y \in V_{\text{row},j}^{\text{MC}}$, and furthermore, $V_{\text{row},j}^{\text{MC}} = \text{span}\{\varphi_j^y\} \oplus \text{span}\{\varphi_{0,K_i^j}\}_{i=1}^m$.

Proof. We present the proof of (a), and omit the proof of (b), which can be obtained similarly. Suppose that $V_{\text{col},i}^{\text{MC}} \neq \emptyset$. Let v_h be a function in $V_{\text{col},i}^{\text{MC}}$. Denote by δ_i the value of v_h on a Gauss point in Figure 9. According to Lemma A.1, it holds on the element K_i^1 that

$$(A.9) \quad \delta_1 - \delta_2 + \delta_4 - \delta_3 = 0;$$

$$(A.10) \quad \theta_1(\delta_1 - \delta_3) + \theta_2(\delta_4 - \delta_2) = 0;$$

$$(A.11) \quad \theta_1(\delta_1 - \delta_2) + \theta_2(\delta_3 - \delta_4) = 0.$$

It follows from (A.9) - (A.11) that $\delta_1 = \delta_2 = \delta_3 = \delta_4$. Apply Lemma A.1 to v_h on K_i^2 , and we obtain $\delta_3 = \delta_4 = \delta_5 = \delta_6$. Repeat the process for the whole row, and we have $\delta_1 = \delta_2 = \dots = \delta_{2n+1} = \delta_{2n+2}$. By definition, it is obvious that $\varphi_i^x \in V_{\text{col},i}^{\text{MC}}$. From Remark A.3, we derive that $V_{\text{col},i}^{\text{MC}} = \text{span}\{\varphi_i^x\} \oplus \text{span}\{\varphi_{0,K_i^j}\}_{j=1}^n$. \square

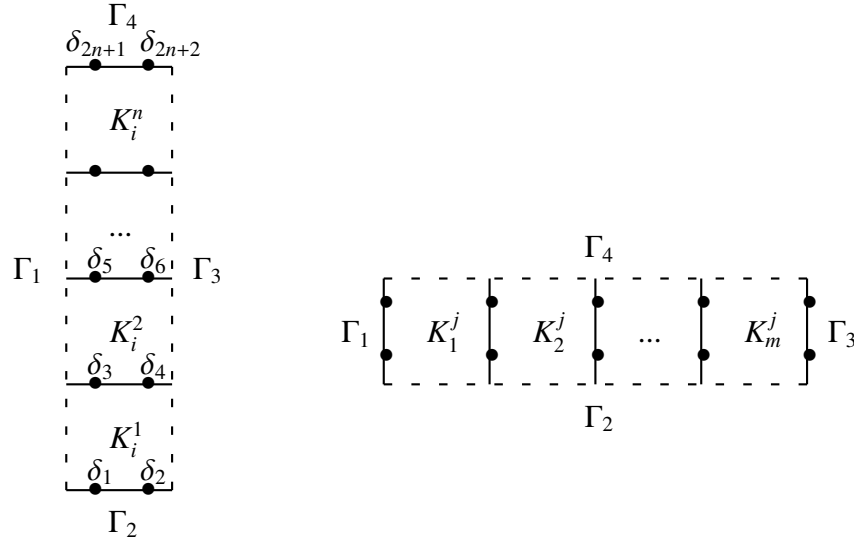


FIGURE 9. Illustration of the column patterns and row patterns of basis functions in V_h^{MC} . These functions vanishes at the Gauss-Legendre points at the dotted lines.

Here and throughout this paper, we do not distinct φ_{0,K_i^j} , $\varphi_{X_i^j}$, φ_i^x , φ_j^y and their respective extension onto the whole domain by zero. Thus we also obtain $\varphi_i^x \in V_h^{\text{MC}}$ and $\varphi_j^y \in V_h^{\text{MC}}$.

A.3. Structure of the MC element space. Here we will present the construction of basis functions in spaces V_{h0}^{MC} and V_h^{MC} .

Theorem A.7. *Let \mathcal{G}_h be a $m \times n$ rectangular subdivision of Ω . Then, $V_{h0}^{\text{MC}} = V_{h0}^{\text{BL}} \oplus \text{span}\{\varphi_{0,K}\}_{K \in \mathcal{G}_h}$.*

Proof. It is obvious that $V_{h0}^{\text{BL}} \cap \text{span}\{\varphi_{0,K}\}_{K \in \mathcal{G}_h} = 0$. We only have to show that $V_{h0}^{\text{MC}} \subset V_{h0}^{\text{BL}} \oplus \text{span}\{\varphi_{0,K}\}_{K \in \mathcal{G}_h}$, i.e., any function in the former is the combination of functions in the latter.

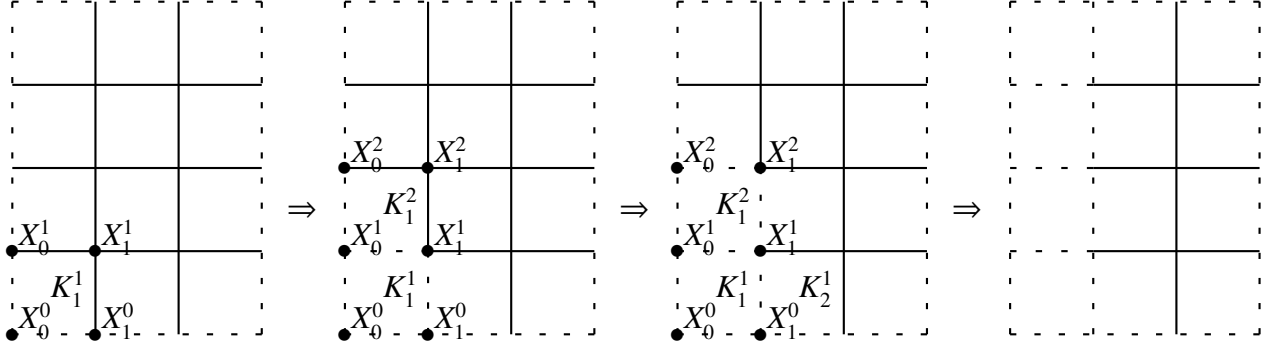


FIGURE 10. Elimination of one column.

Here we use a sweeping procedure. Let $v_h \in V_{h0}^{\text{MC}}$. First, by Lemma A.2, we have that $v_h|_{K_1^1} = \alpha_1^1 \cdot \varphi_{X_1^1}|_{K_1^1} + \gamma_1^1 \cdot \varphi_{0,K_1^1}$ with some constants α_1^1 and γ_1^1 . Therefore, $v_h = v_h^{1,1} + \alpha_1^1 \cdot \varphi_{X_1^1}|_{K_1^1} + \gamma_1^1 \cdot \varphi_{0,K_1^1}$ with $v_h^{1,1} \in V_{h0}^{\text{MC}}$ and $v_h^{1,1}$ vanishing on K_1^1 . Second, $v_h^{1,1} = v_h^{1,2} + \alpha_1^2 \cdot \varphi_{X_1^2} + \gamma_1^2 \varphi_{0,K_1^2}$ with $v_h^{1,2} \in V_{h0}^{\text{MC}}$ and $v_h^{1,2}$ vanishing on K_1^1 and K_1^2 . Furthermore, repeat this process on all the cells of the first column, and we obtain that

$$v_h = v_h^1 + \sum_{j=1}^{n-1} \alpha_1^j \varphi_{X_1^j} + \sum_{j=1}^n \gamma_1^j \varphi_{0,K_1^j},$$

where $v_h^1 \in V_{h0}^{\text{MC}}$ and v_h^1 vanishes on the whole column \mathcal{G}_1 . Finally, we repeat the process from \mathcal{G}_1 to \mathcal{G}_n , and obtain that

$$v_h = \sum_{i=1}^{m-1} \sum_{j=1}^{n-1} \alpha_i^j \varphi_{X_i^j} + \sum_{i=1}^m \sum_{j=1}^n \gamma_i^j \varphi_{0,K_i^j}.$$

Hence the result. \square

Theorem A.8. Let \mathcal{G}_h be a $m \times n$ rectangular subdivision of Ω . Then, we have

$$V_h^{\text{MC}} = V_h^{\text{BL}} + (\text{span}\{\varphi_{0,K}\}_{K \in \mathcal{G}_h} \oplus \text{span}\{\varphi_i^x\}_{i=1}^m \oplus \text{span}\{\varphi_j^y\}_{j=1}^n).$$

Proof. It is obvious that $V_h^{\text{MC}} \supset V_h^{\text{BL}} + (\text{span}\{\varphi_{0,K}\}_{K \in \mathcal{G}_h} \oplus \text{span}\{\varphi_i^x\}_{i=1}^m \oplus \text{span}\{\varphi_j^y\}_{j=1}^n)$. Here we have noted that, if $\varphi_1 + \varphi_2 + \varphi_3 = 0$ with $\varphi_1 \in \text{span}\{\varphi_{0,K}\}_{K \in \mathcal{G}_h}$, $\varphi_2 \in \text{span}\{\varphi_i^x\}_{i=1}^m$, and $\varphi_3 \in \text{span}\{\varphi_j^y\}_{j=1}^n$, then $\varphi_1 = \varphi_2 = \varphi_3 = 0$. We only have to show the other direction. Let $v_h \in V_h^{\text{MC}}$.

First, by (A.8), there exists unique constants $\alpha_0^0, \alpha_0^1, \alpha_1^0, \alpha_1^1, \kappa_1$, and σ_1 , such that

$$v_h|_{K_1^1} = \alpha_0^0 \varphi_{X_0^0}|_{K_1^1} + \alpha_0^1 \varphi_{X_0^1}|_{K_1^1} + \alpha_1^0 \varphi_{X_1^0}|_{K_1^1} + \alpha_1^1 \varphi_{X_1^1}|_{K_1^1} + \kappa_1 \varphi_1^x|_{K_1^1} + \sigma_1 \varphi_1^y|_{K_1^1}.$$

Thus, we have $v_h = v_h^{1,1} + \alpha_0^0 \varphi_{X_0^0} + \alpha_0^1 \varphi_{X_0^1} + \alpha_1^0 \varphi_{X_1^0} + \alpha_1^1 \varphi_{X_1^1} + \kappa_1 \varphi_1^x + \sigma_1 \varphi_1^y$ with $v_h^{1,1} \in V_h^{\text{MC}}$ and $v_h^{1,1}|_{K_1^1} = 0$. Second, by Lemma A.2, we have $v_h^{1,1}|_{K_1^2} = \alpha_0^2 \varphi_{X_0^2}|_{K_1^2} + \alpha_1^2 \varphi_{X_1^2}|_{K_1^2} + \gamma_1^2 \varphi_{0,K_1^2} + \sigma_2 \varphi_2^y|_{K_1^2}$. Therefore, we obtain $v_h^{1,1} = v_h^{1,2} + \alpha_0^2 \varphi_{X_0^2} + \alpha_1^2 \varphi_{X_1^2} + \gamma_1^2 \varphi_{0,K_1^2} + \sigma_2 \varphi_2^y$ with $v_h^{1,2} \in V_h^{\text{MC}}$ and $v_h^{1,2}|_{K_1^1 \cup K_1^2} = 0$.

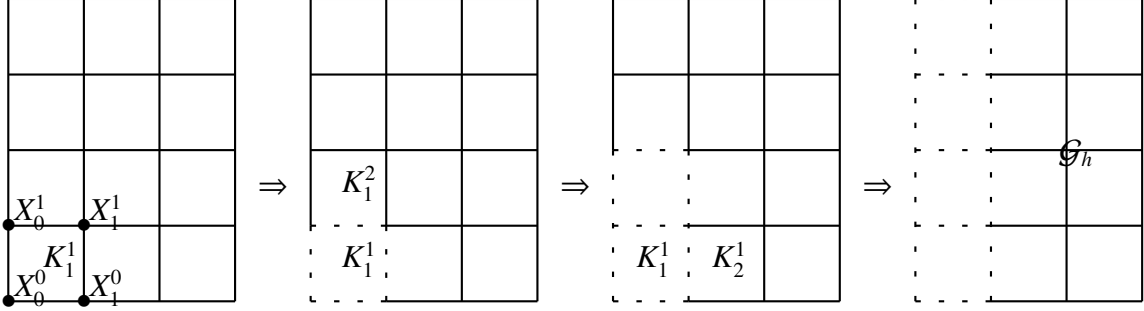


FIGURE 11. Elimination of left column.

Furthermore, repeat this process on the column \mathcal{G}_1 , and we obtain

$$(A.12) \quad v_h = v_h^1 + \sum_{j=0}^n (\alpha_0^j \varphi_{X_0^j} + \alpha_1^j \varphi_{X_1^j}) + \left(\sum_{j=1}^n \gamma_1^j \varphi_{0,K_1^j} \right) - \varphi_{0,K_1^1} + \sum_{j=1}^n \sigma_j \varphi_j^y + \kappa_1 \varphi_1^x,$$

where $v_h^1 \in V_h^{\text{MC}}$ and $v_h^1|_{\mathcal{G}_1} = 0$.

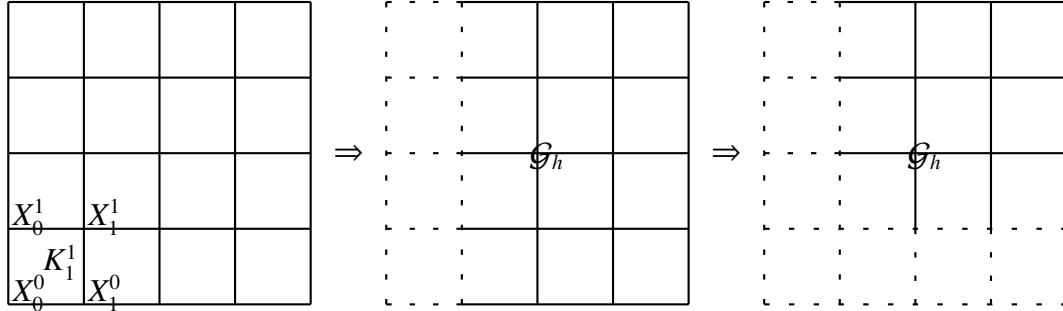


FIGURE 12. Elimination of left column and bottom row.

Similarly, repeat this process on the row \mathcal{G}^1 , and we have

$$(A.13) \quad v_h^1 = \tilde{v}_h^{1,1} + \sum_{i=2}^m (\alpha_i^0 \varphi_{X_i^0} + \alpha_i^1 \varphi_{X_i^1}) + \sum_{i=2}^m \gamma_i^1 \varphi_{0,K_i^1} + \sum_{i=2}^m \kappa_i \varphi_i^x,$$

with $\tilde{v}_h^{1,1} \in V_h^{\text{MC}}$, and $\tilde{v}_h^{1,1}|_{\mathcal{G}_1 \cup \mathcal{G}^1} = 0$. Finally, by the same technique as used in the proof of Theorem A.7, we can prove that

$$(A.14) \quad \tilde{v}_h^{1,1} = \sum_{\substack{2 \leq i \leq m \\ 2 \leq j \leq n}} \alpha_i^j \varphi_{X_i^j} + \sum_{\substack{2 \leq i \leq m \\ 2 \leq j \leq n}} \gamma_i^j \varphi_{0,K_i^j}.$$

A combination of (A.12), (A.13), and (A.14) leads to

$$v_h = \sum_{\substack{0 \leq i \leq m \\ 0 \leq j \leq n}} \alpha_i^j \varphi_{X_i^j} + \left(\sum_{\substack{1 \leq i \leq m \\ 1 \leq j \leq n}} \gamma_i^j \varphi_{0,K_i^j} \right) - \gamma_1^1 \varphi_{0,K_1^1} + \sum_{i=1}^m \kappa_i \varphi_i^x + \sum_{j=1}^n \sigma_j \varphi_j^y.$$

Hence the result. \square

Remark A.9. From the above two theorems, it holds that $\dim(V_{h0}^{\text{MC}}) = 2mn - m - n + 1$ and $\dim(V_h^{\text{MC}}) = 2mn + 2m + 2n$.

Proposition A.10. Define $V_h^{(2)} := \{v_h \in H^1(\Omega) : v_h|_K \in P_2(K), \forall K \in \mathcal{G}_h\}$, and $V_{h0}^{(2)} := V_h^{(2)} \cap H_0^1(\Omega)$.

That is, $V_h^{(2)}$ and $V_{h0}^{(2)}$ are conforming P_2 element spaces. Then,

- (1) $V_h^{(2)} = V_h^{\text{BL}} + \text{span}\{\varphi_i^x, \varphi_j^y\}$, and $V_{h0}^{(2)} = V_{h0}^{\text{BL}}$;
- (2) $V_h^{\text{MC}} = V_h^{(2)} + \text{span}\{\varphi_{0,K}\}_{K \in \mathcal{G}_h}$, and $V_{h0}^{\text{MC}} = V_{h0}^{(2)} + \text{span}\{\varphi_{0,K}\}_{K \in \mathcal{G}_h}$.

Proposition A.11. Let V_h^{W} be the Wilson element space and V_{h0}^{W} be its homogeneous subspace.

Then

- (1) $\nabla_h V_h^{\text{MC}} \subset \nabla_h V_h^{\text{W}}$, and $\nabla_h V_{h0}^{\text{MC}} \subset \nabla_h V_{h0}^{\text{W}}$;
- (2) $V_h^{\text{MC}} \setminus V_h^{\text{W}} \neq \emptyset$, $V_h^{\text{W}} \setminus V_h^{\text{MC}} \neq \emptyset$, $V_{h0}^{\text{MC}} \setminus V_{h0}^{\text{W}} \neq \emptyset$, and $V_{h0}^{\text{W}} \setminus V_{h0}^{\text{MC}} \neq \emptyset$.

APPENDIX B. CONSTRUCTION OF BASIS FUNCTIONS FOR THE REDUCED RECTANGULAR MORLEY (RRM) ELEMENT SPACE

Let $\Omega \in \mathbb{R}^2$ be rectangle domain divided by $m \times n$ rectangles. Define the reduced rectangular Morley element spaces as

$$(B.1) \quad V_h^{\text{R}} := \left\{ w \in L^2(\Omega) : w|_K \in P_2(K), w_h(a) \text{ is continuous at } a \in \mathcal{N}_h^i, \text{ and } \int_e \partial_{n_e} w_h ds \text{ is continuous across } e \in \mathcal{E}_h^i \right\};$$

$$(B.2) \quad V_{hs}^{\text{R}} := \left\{ w_h \in V_h^{\text{R}} : w_h(a) \text{ vanishes at } a \in \mathcal{N}_h^b \right\}.$$

In this section, we will present an available set of basis functions of V_{hs}^{R} .

B.1. Compatibility conditions. By a pure linear algebra argument, the following description holds for $P_2(K)$.

Lemma B.1. ([36, Lemma 15]) *Let K be a rectangle with vertices a_i and edges Γ_l ($i, l = 1 : 4$). Denote its length and width by L and H , respectively; see Figure 13 (Left). Then, given $\alpha_i, \beta_i \in \mathbb{R}$,*

there exists a uniquely $p \in P_2(K)$ satisfying

$$p(a_i) = \alpha_i, \oint_{\Gamma_1} \partial_x p = \beta_1, \oint_{\Gamma_2} \partial_y p = \beta_2, \oint_{\Gamma_3} \partial_x p = \beta_3, \oint_{\Gamma_4} \partial_y p = \beta_4.$$

if and only if the following compatibility conditions are satisfied on K ,

$$(B.3) \quad \frac{\alpha_3 - \alpha_4}{L} + \frac{\alpha_2 - \alpha_1}{L} = \beta_1 + \beta_3;$$

$$(B.4) \quad \frac{\alpha_3 - \alpha_2}{H} + \frac{\alpha_4 - \alpha_1}{H} = \beta_2 + \beta_4.$$

Recall the definitions of \mathcal{G}_h , \mathcal{G}_i , and \mathcal{G}^j in Appendix A. Also, the vertices are labeled by X_i^j , the midpoints on any edge by Y_i^j and Z_i^j , and the cells by K_i^j ; see Figure 13 (Right). Next we present some local or global functions in V_{hs}^R by giving their value on $X_i^j \in \mathcal{E}_h^i$ and derivative on the midpoint of $e \in \mathcal{E}_h$.

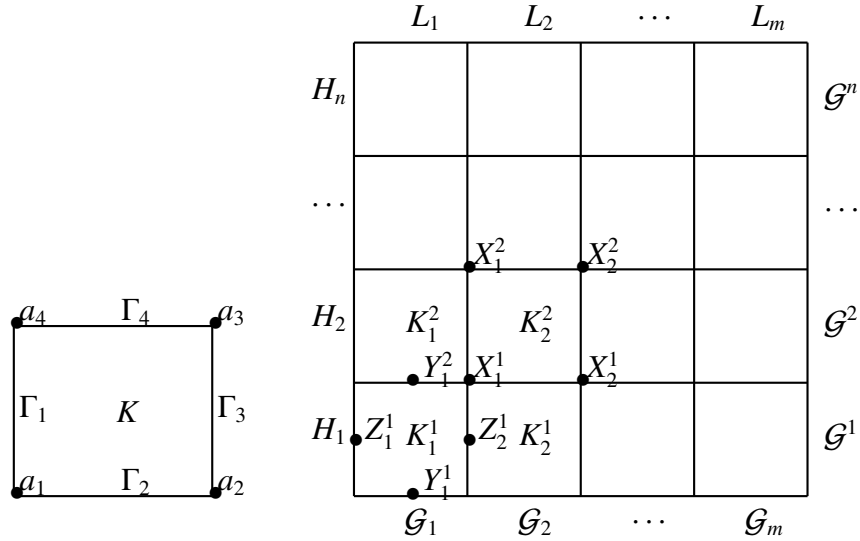


FIGURE 13. Left: Illustration of a rectangle K with width L and height H . Right: Illustration of the grid \mathcal{G}_h : X_i^j denotes the vertices, Y_i^j and Z_i^j denote the midpoints and K_i^j denotes the cells. L_i and H_i denote the widths (heights) of the cells in the same column (row).

B.2. Patterns of supports of basis functions in V_{hs}^R . Associated with \mathcal{G}_h , we present some patterns, i.e., the support sets of basis functions in the RRM element space. To begin with, we introduce some notations. An interior edge, denoted by $e_{\text{bot},i}$ ($2 \leq i \leq m-1$), is called a bottom interior edge if its two endpoints are interior points, and its lower opposite edge is on the bottom of \mathcal{G}_h . A top interior edge $e_{\text{top},i}$, a left interior edge $e_{\text{lef},j}$, and a right interior edge $e_{\text{rig},j}$ are defined in a similar way ($2 \leq j \leq n-1$).

In the following lemmas, we always denote, by ω , a generic patch with boundaries Γ_l ($l = 1 : 4$), anticlockwise.

Lemma B.2. *Let $e_{\text{bot},i}$ ($2 \leq i \leq m-1$) be a bottom interior edge with endpoints X_{i-1}^1 and X_i^1 . Let ω be a 3×2 cells patch as shown in Figure 14, left. Define*

$$V_{\text{bot},i}^{\text{R}} := \left\{ v_h \in V_{hs}^{\text{R}}(\omega) : \int_e \partial_{n_e} v_h ds = 0, \forall e \subset \Gamma_l, l = 1, 3, 4 \right\}.$$

Likewise, we can define $V_{\text{top},i}^{\text{R}}$ (see Figure 14, right), $V_{\text{lef},j}^{\text{R}}$ and $V_{\text{rig},j}^{\text{R}}$ (see Figure 15, left and right), where $2 \leq i \leq m-1$ and $2 \leq j \leq n-1$. Then we have $\dim(V_{\text{bot},i}^{\text{R}}) = \dim(V_{\text{top},i}^{\text{R}}) = \dim(V_{\text{lef},j}^{\text{R}}) = \dim(V_{\text{rig},j}^{\text{R}}) = 1$.

Proof. First, we consider $V_{\text{bot},i}^{\text{R}}$. Let the geometric features of ω be represented as in Figure 14, left. Given $\varphi \in V_{\text{bot},i}^{\text{R}}$, denote by $x_i^j := \varphi(X_i^j)$, $y_i^j := \partial_y \varphi(Y_i^j)$, and $z_i^j := \partial_x \varphi(Z_i^j)$. Apply conditions (B.3) and (B.4) on every element, we have, row by row,

$$(B.5) \quad \frac{x_{i-1}^1}{L_{i-1}} = z_i^1, \quad \frac{x_{i-1}^1}{H_1} = y_{i-1}^1 + y_{i-1}^2, \quad \frac{x_i^1 - x_{i-1}^1}{L_i} = z_i^1 + z_{i+1}^1, \quad \frac{x_i^1 + x_{i-1}^1}{H_1} = y_i^1 + y_i^2,$$

$$(B.6) \quad -\frac{x_i^1}{L_{i+1}} = z_{i+1}^1, \quad \frac{x_i^1}{H_1} = y_{i+1}^1 + y_{i+1}^2, \quad \frac{x_{i-1}^1}{L_{i-1}} = z_i^2, \quad -\frac{x_{i-1}^1}{H_2} = y_{i-1}^2,$$

$$(B.7) \quad \frac{x_i^1 - x_{i-1}^1}{L_i} = z_i^2 + z_{i+1}^2, \quad -\frac{x_{i-1}^1 + x_i^1}{H_2} = y_i^2, \quad -\frac{x_i^1}{L_{i+1}} = z_{i+1}^2, \quad -\frac{x_i^1}{H_2} = y_{i+1}^2.$$

Rewrite the system after adjusting the order,

$$(B.8) \quad \frac{1}{L_{i-1}} x_{i-1}^1 - z_i^1 = 0,$$

$$(B.9) \quad \frac{1}{H_1} x_{i-1}^1 - y_{i-1}^1 - y_{i-1}^2 = 0,$$

$$(B.10) \quad -\frac{1}{L_i} x_{i-1}^1 + \frac{1}{L_i} x_i^1 - z_i^1 - z_{i+1}^1 = 0,$$

$$(B.11) \quad \frac{1}{H_1} x_{i-1}^1 + \frac{1}{H_1} x_i^1 - y_i^1 - y_i^2 = 0,$$

$$(B.12) \quad -\frac{1}{L_{i+1}} x_i^1 - z_{i+1}^1 = 0,$$

$$(B.13) \quad \frac{1}{H_1} x_i^1 - y_{i+1}^1 - y_{i+1}^2 = 0,$$

$$(B.14) \quad \frac{1}{L_{i-1}} x_{i-1}^1 - z_i^2 = 0,$$

$$(B.15) \quad -\frac{1}{H_2} x_{i-1}^1 - y_{i-1}^2 = 0,$$

$$(B.16) \quad -\frac{1}{L_i} x_{i-1}^1 + \frac{1}{L_i} x_i^1 - z_i^2 - z_{i+1}^2 = 0,$$

$$(B.17) \quad -\frac{1}{H_2} x_{i-1}^1 - \frac{1}{H_2} x_i^1 - y_i^2 = 0,$$

$$(B.18) \quad -\frac{1}{L_{i+1}} x_i^1 - z_{i+1}^2 = 0,$$

$$(B.19) \quad -\frac{1}{H_2} x_i^1 - y_{i+1}^2 = 0.$$

It is straightforward to verify that (B.10) – (B.8) – (B.12) – [(B.16) – (B.14) – (B.18)] = 0. The system admits a one-dimension solution space. Thus we obtain $\dim(V_{\text{bot},i}^{\text{R}}) = 1$. Likewise, we have $\dim(V_{\text{top},i}^{\text{R}}) = \dim(V_{\text{lef},j}^{\text{R}}) = \dim(V_{\text{rig},j}^{\text{R}}) = 1$ ($\forall 2 \leq i \leq m-1, 2 \leq j \leq n-1$). \square

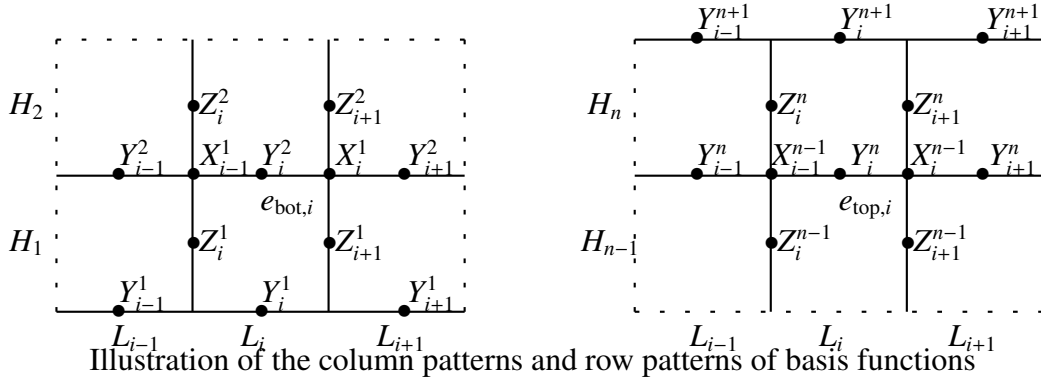


FIGURE 14. Left: Illustration of a 3×2 pattern associated with e_{bot}^i . Right: Illustration of a 3×2 pattern associated with $e_{\text{top},i}$. The values or derivatives vanish at edges on the dotted lines.

With similar procedures in Lemma B.3, the following two lemmas can be obtained.

Lemma B.3. *Let X_{m-1}^{n-1} be an interior node in the northeast corner. Let ω be a 2×2 patch as shown in Figure 16, left. Define $V_X^{\text{R}} := \{v_h \in V_{hs}^{\text{R}}(\omega) : \int_e \partial_{n_e} v_h ds = 0, \forall e \subset \Gamma_l (l = 1, 2)\}$. Then $\dim(V_X^{\text{R}}) = 1$.*

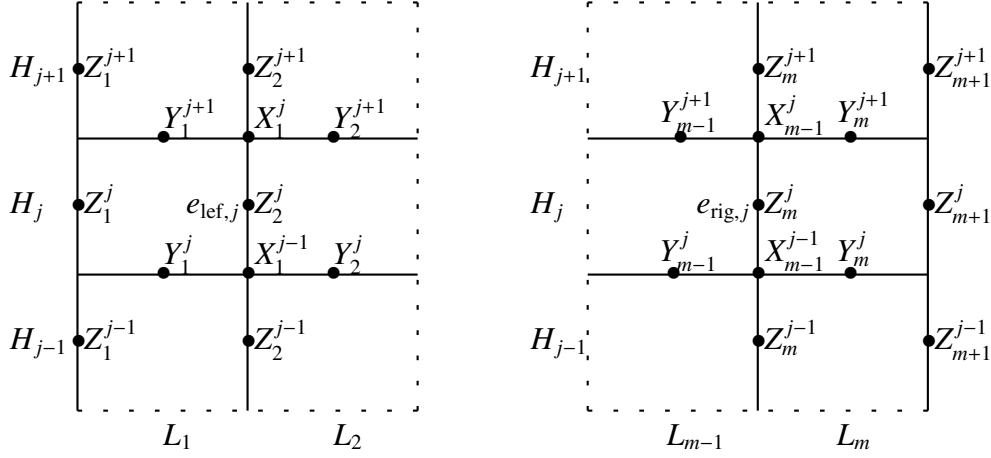


FIGURE 15. Left: Illustration of a 2×3 pattern associated with $e_{\text{lef},j}$. Right: Illustration of a 2×3 pattern associated with $e_{\text{rig},j}$. The values or derivatives vanish at edges on the dotted lines.

Lemma B.4. ([36, Lemma 15]) *Let ω be a 3×3 patch as shown in Figure 16, right. Define*

$$V_{K_i^j}^{\text{R}} := \left\{ v_h \in V_{hs}^{\text{R}}(\omega) : \int_e \partial_{n_e} v_h ds = 0, \forall e \subset \Gamma_i (1 \leq l \leq 4) \right\}, \text{ where } 2 \leq i \leq m-1 \text{ and } 2 \leq j \leq n-1.$$

Then $\dim(V_{K_i^j}^{\text{R}}) = 1$.

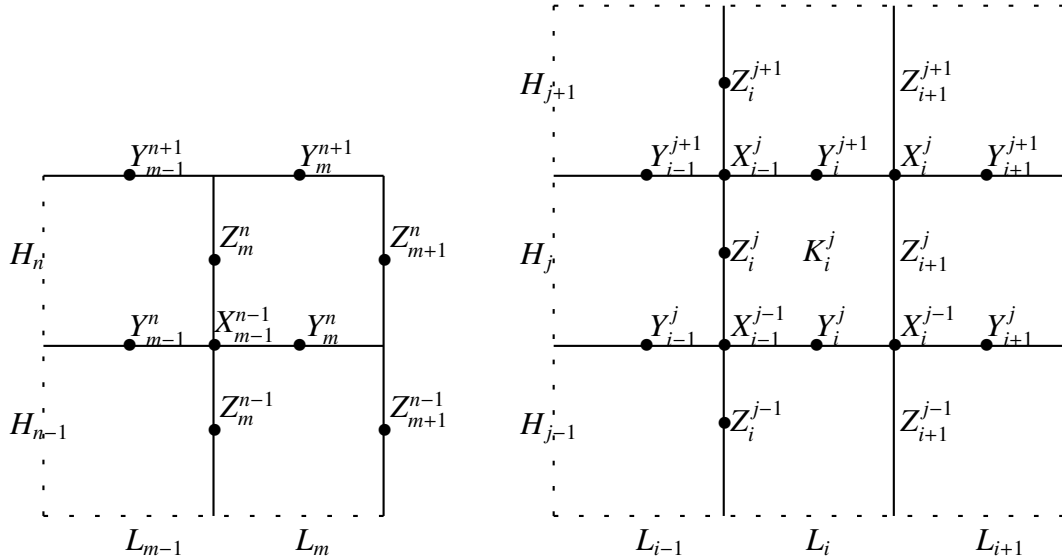


FIGURE 16. Left: Illustration of a 2×2 pattern associated with X_{m-1}^{n-1} . Right: Illustration of a 3×3 pattern associated with K_i^j . The values or derivatives vanish at edges on the dotted lines.

Lemma B.5. *Let ω be a 3×1 or 1×3 patch in Figure 17, left and right, respectively. Define*

$$V_\omega := \left\{ v_h \in V_{hs}^R(\omega) : \int_e \partial_{n_e} v_h ds = 0, \forall e \subset \Gamma_l (l = 1, 2, 3) \right\}.$$

Then, $\dim(V_\omega) = 1$ and $v_h(X_1) = 0$ implies $v_h \equiv 0$ on ω .

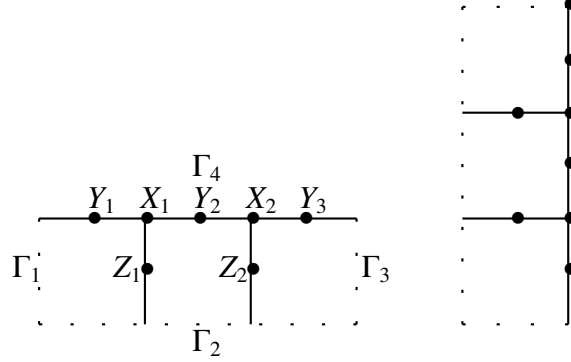


FIGURE 17. Illustration of 3×1 or 1×3 patch ω . The values or derivatives vanish at edges on the dotted lines.

Lemma B.6. *If we denote $\omega = \mathcal{G}_i$ the union of elements in the i -th column with boundaries $\bigcup_{l=1}^4 \Gamma_l$ (see Figure 18, left), and define*

$$V_{\text{col},i}^R := \left\{ v_h \in V_{hs}^R(\omega) : \int_e \partial_{n_e} v_h ds = 0, \forall e \subset \Gamma_l (l = 1, 3) \right\},$$

then $\dim(V_{\text{col},i}^R) = 1$. If $\omega = \mathcal{G}^j$ (see Figure 18, right), and define

$$V_{\text{row},j}^R := \left\{ v_h \in V_{hs}^R(\omega) : \int_e \partial_{n_e} v_h ds = 0, \forall e \subset \Gamma_l (l = 2, 4) \right\},$$

then $\dim(V_{\text{row},j}^R) = 1$.

Proof. Obviously, $V_{\text{col},i}^R \neq \emptyset$. Assume that $v_h \in V_{\text{col},i}^R$. We denote $y_i^j := v_h(Y_i^j)$, where $1 \leq j \leq n+1$; see Figure 18 (Left). Apply (B.3) and (B.4) to v_h on each element in \mathcal{G}_i , and we obtain $y_i^j = -y_i^{j+1}$ ($1 \leq j \leq n$). It proves that $\dim(V_{\text{col},i}^R) = 1$. Similarly, assume that $w_h \in V_{\text{col},i}^R$ and denote $z_i^j := w_h(Z_i^j)$ ($1 \leq i \leq m+1$). We have $z_i^j = -z_{i+1}^j$ ($1 \leq i \leq m$); see Figure 18 (Right). Thus we obtain $\dim(V_{\text{row},j}^R) = 1$. \square

Remark B.7. Here and throughout this paper, we do not distinct between $V_{\text{bot},i}^R$, $V_{\text{top},i}^R$, $V_{\text{lef},j}^R$, $V_{\text{rig},j}^R$, V_X^R , $V_{K_i^j}^R$, $V_{\text{col},i}^R$, $V_{\text{row},j}^R$ and their respective extension onto the whole domain by zero. Each of them is a subspace in V_{hs}^R .

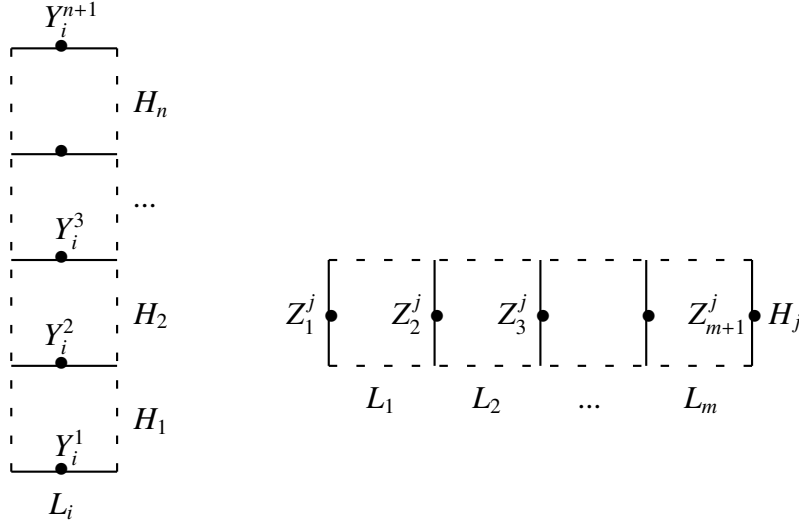


FIGURE 18. Left: Illustration of a column pattern associated with \mathcal{G}_i . Right: Illustration of a row pattern associated with \mathcal{G}^j . The values or derivatives vanish at edges on the dotted lines.

B.3. Structure of the RRM element space.

Theorem B.8. Let \mathcal{G}_h be a $m \times n$ rectangular subdivision of Ω . Define $V_{bltr}^R := \oplus_{i,j} (V_{bot,i}^R \oplus V_{top,i}^R \oplus V_{lef,j}^R \oplus V_{rig,j}^R)$, $V_K^R := \oplus_{i,j} V_{K_i^j}^R$, and $V_{glob}^R := V_{col,m-1}^R \oplus V_{col,m}^R \oplus V_{row,n-1}^R \oplus V_{row,n}^R$, where $2 \leq i \leq m-1$, and $2 \leq j \leq n-1$. Then we have $V_{hs}^R = V_{bltr}^R \oplus V_{glob}^R \oplus V_K^R \oplus V_X^R$.

Proof. Here we utilize the sweeping procedure again, and divide the proof process into four steps.

Step 1. Given $v \in V_{hs}^R$. We begin with the boundaries of \mathcal{G}_h ; see Figure 19. Recall the definition of $e_{bot,i}$, $e_{top,i}$, $e_{lef,j}$, and $e_{rig,j}$. Associated with $e_{bot,2}$, $V_{bot,2}^R$ is a subspace of V defined in Lemma B.2. There exists a unique function $\varphi_{b,1} \in V_{bot,2}^R$, such that $\varphi_{b,1}(Y_1^1) = v(Y_1^1)$. Then, $v_1 = v - \varphi_{b,1}$ with $v_1 \equiv 0$ on the bottom edge of K_1^1 . Repeat the procedure for Y_2^1, \dots, Y_{m-2}^1 , and we obtain $v_{m-2} = v - \sum_{i=2}^{m-1} \varphi_{b,i}$ with v_{m-2} vanishing on the first $m-2$ edges on the bottom boundary of \mathcal{G}_h . Similarly, we obtain functions $\varphi_{t,i}$, $\varphi_{l,j}$, and $\varphi_{r,j}$. Therefore, $w_1 = v - \sum_{i=2}^{m-1} \varphi_{b,i} - \sum_{i=2}^{m-1} \varphi_{t,i} - \sum_{j=2}^{n-1} \varphi_{l,j} - \sum_{j=2}^{n-1} \varphi_{r,j}$ with w_1 vanishing on the dotted edges; see Figure 19 (Middle).

Step 2. There exists uniquely $\varphi_{col,i}$ in $V_{col,i}^R$ and $\varphi_{row,j}$ in $V_{row,j}^R$, which satisfy $\varphi_{col,i}(Y_i^1) = w_1(Y_i^1)$, and $\varphi_{row,j}(Z_1^j) = w_1(Z_1^j)$, respectively. Then $w_2 = w_1 - \sum_{i=m-1}^m \varphi_{col,i} - \sum_{j=n-1}^n \varphi_{row,j}$ with w_2 vanishing on the dotted edges; see Figure 19 (Right).

Step 3. Consider elements in the first column \mathcal{G}_1 ; see Figure 17. Note that K_2^2 is the only interior element whose 3×3 patch contains K_1^1 . There exists uniquely $\varphi_1^1 \in V_{K_2^2}^R$, such that $\varphi_1^1|_{K_1^1} = w_2|_{K_1^1}$.

Therefore, $w_2 - \varphi_1^1$ vanishes on K_1^1 . Next, there exists a unique $\varphi_1^2 \in V_{K_2^2}^{\mathbb{R}}$, such that $w_2 - \varphi_1^1 - \varphi_1^2$ vanishes on $K_1^1 \cup K_1^2$. Repeating the procedure for \mathcal{G}_1 , we obtain $w_2 - \sum_{j=1}^{n-2} \varphi_1^j$, which vanishes on $\cup_{j=1}^{n-2} K_1^j$. Notice that $\cup_{j=1}^{n-2} K_1^j$ is a 1×3 patch ω stated in Lemma B.5; see Figure 20 (Left). Since $w_2 - \sum_{j=1}^{n-2} \varphi_1^j$ vanishes on X_1^{n-2} , it vanishes on ω and further \mathcal{G}_1 .

By repeating the procedure along the column \mathcal{G}_i ($i = 2, \dots, m-2$), we derive $w_3 := w_2 - \sum_{i=1}^{m-2} \sum_{j=1}^{n-2} \varphi_i^j$, which vanishes on $\cup_{i=1}^{m-2} \mathcal{G}_i$. Especially, $w_3(X_{m-2}^j) = 0$ ($1 \leq j \leq n-2$). Since $\cup_{i=m-2}^m K_i^1$ forms a 1×3 patch ω (see Figure 20, middle) and $w_3(X_{m-2}^1) = 0$, thus it vanishes on ω . Find other 1×3 or 3×1 patch ω , which satisfies the conditions in Lemma B.5, in columns \mathcal{G}_{m-2} , \mathcal{G}_{m-1} , and \mathcal{G}_m . Therefore, we derive that w_3 vanishes on \mathcal{G}_h except for a 2×2 patch in the northeast corner; see Figure 20 (Right).

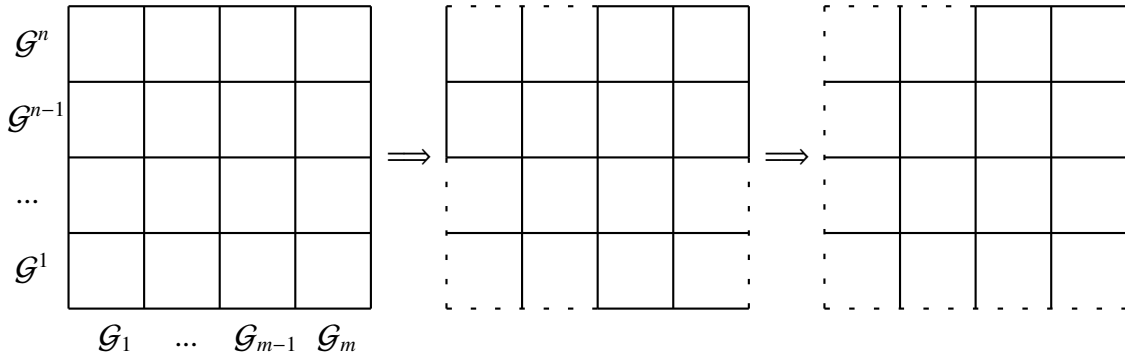


FIGURE 19. Elimination process of Step 1 and 2.

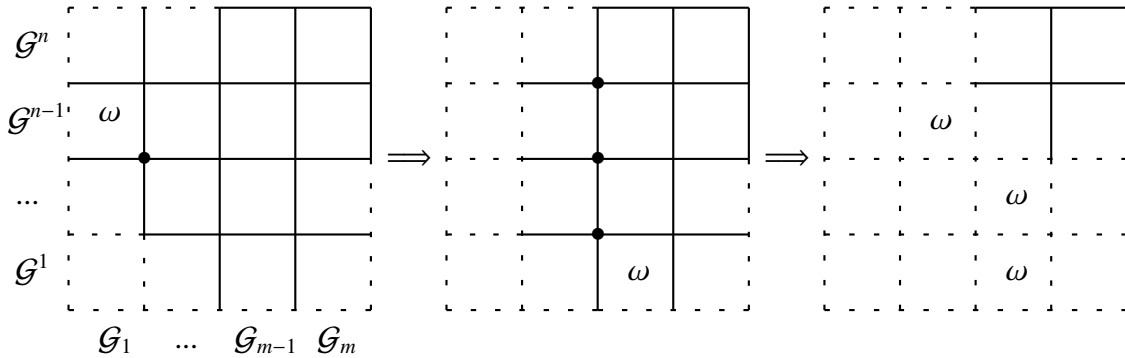


FIGURE 20. Elimination process of Step 3 and 4.

Step 4. From Lemma B.3, there exists a unique function $\varphi_{m-1}^{n-1} \in V_X^{\mathbb{R}}$ and $w_3 - \varphi_{m-1}^{n-1} = 0$. This way, we have verified that $v = (\sum_{i=2}^{m-1} \varphi_{b,i} + \sum_{i=2}^{m-1} \varphi_{t,i} + \sum_{j=2}^{n-1} \varphi_{l,j} + \sum_{j=2}^{n-1} \varphi_{r,j}) + (\sum_{i=m-1}^m \varphi_{\text{col},i} + \sum_{j=n-1}^n \varphi_{\text{row},j}) + \sum_{i=1}^{m-2} \sum_{j=1}^{n-2} \varphi_i^j + \varphi_{m-1}^{n-1}$, and this representation by these $mn + 1$ functions is unique. \square

Remark B.9. From Theorem B.8, it holds that $\dim V_{hs}^R = mn + 1$.

Proposition B.10. It holds for $V_h^W, V_{h0}^W, V_h^M, V_{hs}^M, V_h^R$, and V_{hs}^R that

$$(B.20) \quad V_h^R = V_h^M \cap V_h^W;$$

$$(B.21) \quad V_{hs}^R = V_{hs}^M \cap V_{h0}^W.$$

LSEC, ICMSEC, ACADEMY OF MATHEMATICS AND SYSTEM SCIENCES, CHINESE ACADEMY OF SCIENCES, BEIJING 100190, CHINA; SCHOOL OF MATHEMATICAL SCIENCES, UNIVERSITY OF CHINESE ACADEMY OF SCIENCES, BEIJING 100049, CHINA

E-mail address: zhl@lsec.cc.ac.cn

LSEC, ICMSEC AND NCMIS, ACADEMY OF MATHEMATICS AND SYSTEM SCIENCES, CHINESE ACADEMY OF SCIENCES, BEIJING 100190, CHINA

E-mail address: zhangcs@lsec.cc.ac.cn

LSEC, ICMSEC AND NCMIS, ACADEMY OF MATHEMATICS AND SYSTEM SCIENCES, CHINESE ACADEMY OF SCIENCES, BEIJING 100190, CHINA

E-mail address: szhang@lsec.cc.ac.cn